Unravelling the role of precursors phosphine`s features in governing the reactivity of [MCl_2(P-P)] (M = Pd, Pt) towards formation of thiolate complexes via S−S and S−C bond cleavage

Saili Vikram Lokhande[a], Sandeep Nigam[b], Afsar Ali Siddiki[a], Raymond J. Butcher[c], Rohit Singh Chauhan[a*], Adish Tyagi[b]

[a] *Department of Chemistry, K. J. Somaiya College of Science and Commerce, Vidyavihar, Mumbai 400077, India.*

[b] *Chemistry Division, Bhabha Atomic Research Centre, Mumbai 400085, Homi Bhabha National Institute, Mumbai 400 094, India.*

[c] *Department of Chemistry, Howard University, Washington DC, 20059, United States.*

Email: rohit.chauhan@somaiya.edu

Abstract:

Group 10 thiolate complexes have been in the quest zone of research due to pertinent catalytic potential. The present work unravels the role of precursor phosphine`s feature in their reactivity towards 4,6-dimethyl pyrimidine-2-thiol and subsequent thiolate complex. Synthesized thiolate complexes were thoroughly characterized using elemental analyses, NMR (^1H, $^{13}C\{^1H\}$, $^{31}P\{^1H\}$), UV-Vis spectroscopy and Single Crystal X-ray diffraction analyses. Treatment of [$MCl_2(PPh_3)_2$] (M = Pd, Pt) with two equivalents of $NaSC_4H(4,6\text{-}Me)N_2$ resulted in chelated [Pd{κ-S, κ-N: $SC_4H(4,6\text{-}Me)_2N_2$}{$SC_4H(4,6\text{-}Me)_2N_2$}($PPh_3$)] (**1a**) as well as an expected *trans* compound [Pt{$SC_4H(4,6\text{-}Me)_2N_2$}$_2$($PPh_3$)$_2$] (**1b**). A similar reaction with the chelating phosphine 'dppm' (dppm = 1,1-bis(diphenylphosphino)methane) as an ancillary ligand resulted in the serendipitous product of composition [Pd_2(μ_2-S){$SC_4H(4,6\text{-}Me)_2N_2$}$_2$($\mu_2$-dppm)$_2$] (**2a**) depending upon competitive cleavage of S-S and S-C bond. The reaction of [$PdCl_2$(dppe)] afforded a *cis* configured compound [Pd{2-SC_4H(4,6-

Me)$_2$N$_2$}$_2$(dppe)] (**2b**). Contrary, the similar reaction of [PdCl$_2$(dppp)] results in removal of 'dppp' (1,3-bis(diphenylphosphino)propane) yielding the chelated complex [Pd{κ-S, κ-N: SC$_4$H(4,6-Me)$_2$N$_2$}$_2$] (**2c**). Above all, the reactivity of 4,6-dimethyl pyrimidine-2-thiol significantly differs compared to unsubstituted pyrimidyl, pyridyl analogue which has been attributed to the additional richness of electrons/activation in the ring which in turn facilitates competitive reactivity pattern of S-S and S-C bond. The virtue of such activation can easily be understood by the isolation of complex [Pd$_2$(μ_2-S){SC$_4$H(4,6-Me$_2$)$_2$N$_2$}$_2$(μ_2-dppm)$_2$] (**2a**). Rationalization of results via DFT calculation reveals that projection angle P-M-P (ranging from ~75 to 92°) driven structural change in the chelating phosphine and associated degree of softness in ligand molecule played a crucial role in governing the resulting product of substitution reaction as dimeric, monomeric and chelated complexes. Thus, projection angle-driven geometrical and electronic structure and variation provide opportunity and direction to efficiently derive biologically as well as academically important complexes.

Keywords: tertiary phosphines, thiolates, NMR, DFT, crystallography.

1. Introduction:

Significant attention has been perceived towards group 10 metal chalcogenolate complexes derived from hybrid ligands due to their structural diversification and rich coordination chemistry [1-6]. Numerous applications of these complexes in the domain of catalysis [7-10] and material science [11, 12] have made this field quite evolving. Among them, palladium and platinum thiolate complexes have extensively been used as molecular precursors for the synthesis of metal chalcogenide (ME) nanomaterials of different compositions such as PdSe, Pd$_{4.5}$Se, Pd$_{17}$Se$_{15}$ which displayed excellent activity for hydrogen evolution reaction [13] and counter electrode in dye-sensitized solar cells [14].

Jain et al., have studied the reaction of [PtCl$_2$(PPh$_3$)$_2$] with the sodium salt of pyridylthiolate resulting in monomeric complex *trans*-[Pt(Spy)$_2$(PPh$_3$)$_2$] [15]. In the same continuation, a series of palladium complexes derived from S, N-chelating heterocyclic thionate ligands having composition $[Pd(Ar)(PPh_3)_2](ClO_4)$ [Ar = pyridine-2-thiolate, pyrimidine-2-thiolate, imidazolidine-2-thiolate, 1-methylimidazoline-2-thiolate and 1,3-thiazoline-2-thiolate] [16] have been investigated. The *cis* configured compounds $[M(\eta^1\text{-S-}C_5H_4NS)_2(P\text{-}P)]$ (M = Pd, Pt) [P-P = dppe (1,2-bis(diphenylphosphino)ethane), dppp (1,3-bis(diphenylphosphino)propane)] were synthesized by reacting pyridine-2-thione with corresponding metal substrates [17]. To extend this category, Pt metallacycles $[(P\text{-}P)Pt(\mu\text{-py-}E)]_n(X)_n$ (n = 2 or 4, E = S or Se, X = OTf (trifluoromethanesulfonate) or BPh_4 (tetraphenylborate); P-P = dppe (1,2-bis(diphenylphosphino)ethane), dppf (1,1′-bis(diphenylphosphino)ferrocene)] based on 4-pyridylthiolate/selenolate and chelating phosphines (dppe, dppf) showed a promising anticancer activity [18]. An introduction of one more nitrogen in pyridyl backbone i.e. pyrimidine enhanced the reactivity to manifold, resulted in several products $[M(S\text{-}C_4H_3SN_2)_2(dppe)]$ [M = Pd, Pt], $[Pd(S\text{-}C_4H_3SN_2)_2(dppm)_2]$, $[Pt(S\text{-}C_4H_3SN_2)_2(dppm)]$ as well as byproducts such as $[Pd_2(S\text{-}N\text{-}C_4H_3SN_2)_4]$ and *trans*-$[Pt(S\text{-}C_4H_3SN_2)(PPh_2Me)_2]$ [19]. Isolation of these complexes depends upon the nature of phosphine. However, the chemistry of higher congeners is quite different compared to the thiol ligand systems. For instance oxidative addition of $\{Se\text{-}C_5H_3(3\text{-}R)N\}_2$ (R = H or Me) to $[Pd(P\text{-}P)_2]$ (P-P = dppe, dppp) yielded a mononuclear complex $[Pd(2\text{-}Se\text{-}C_5H_3(3\text{-}R)N)_2(P\text{-}P)]$ [P-P/R = dppe/H or Me; dppp/H) as well as a binuclear complex $[Pd_2(\mu\text{-}SeC_5H_3(3\text{-}Me)N)_2(dppp)]^{2+}$ (R = Me) whereas pyridyl and pyrimidyl ditellurides afforded exclusively trinuclear complex having composition $[Pd_3(\mu\text{-}Te)_2(P\text{-}P)_3]Cl_2$ (P-P = dppe, dppp) [20].

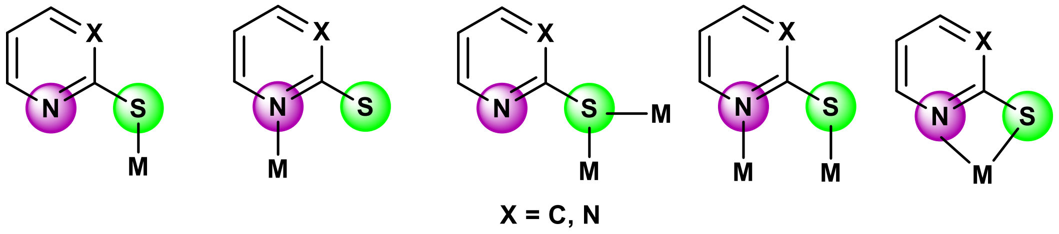

Figure 1: Bonding modes in heterocyclic thiolate ligands (redrawn from the reference 6, 12)

An adaptable coordination tendency of internally functionalized heterocyclic thiolate ligands assists in obtaining a variety of novel metal thiolate complexes. These ligand systems can coordinate a metal atom in several modes (**Figure 1**) such as only through sulfur atom, nitrogen atom or both donor atoms in bidentate fashion (chelating or bridging) [1, 12, 21]. The current study elucidates the function of phosphine in the reactivity between 4,6-dimethyl pyrimidin-2-thiolate and $[MCl_2(P\text{-}P)]$ (M = Pd, Pt and P-P = PPh_3, dppe, dppm, dppp). The details of our findings are described herein.

2. Experimental:

2.1 Materials and Methods

All the reactions were carried out under a nitrogen atmosphere using standard Schlenk line techniques. Solvents applied during the course of reaction were distilled by standard protocols [22]. Palladium(II) chloride, tris(dibenzylideneacetone)dipalladium, potassium tetrachloroplatinate, triphenylphosphine, 1,1-bis(diphenylphosphino)methane (dppm), 1,2-bis(diphenylphosphino)ethane (dppe), 1,3-bis(diphenylphosphino)propane (dppp), sodium borohydride were procured from Sigma Aldrich and applied without any purification. The metal precursors $[MCl_2(P\text{-}P)_2]$ (M = Pd, Pt; P-P = PPh_3, dppm, dppe, dppp) [23] and the ligands bis-4,6-dimethyl pyrimidin-2-yl disulfide were synthesized as reported in the literature [24]. Elemental analyses were carried out on a Flash smart V CHNS analyser. UV-visible absorption spectra were recorded with the help of an Agilent 81 Technologies Carry 60 single beam spectrophotometer. The NMR ^1H, $^{13}C\{^1H\}$, $^{31}P\{^1H\}$ spectra were recorded on Bruker Avance-II 78 spectrometer operating at a scanning frequency of 300, 75, 121.44 MHz respectively and referenced for the solvent peak of chloroform at δ 7.25 for ^1H and externally to 85% phosphoric acid (0.00 ppm) for $^{31}P\{^1H\}$ NMR.

The single crystal X-ray data for $[Pd\{\kappa\text{-}S, \kappa\text{-}N: SC_4H(4,6\text{-}Me)_2N_2\}\{SC_4H(4,6\text{-}Me)_2N_2\}(PPh_3)]$ (**1a**) was collected using Rigaku Oxford Diffraction Synergy S equipped with a micro-focus sealed X-ray tube, Cu-Kα (λ = 1.54184 Å). However, the data for [Pt{$SC_4H(4,6-Me)_2N_2$}$_2$(PPh_3)$_2$].$2C_6H_6$.$2CH_3CN$ (**1b**), [Pd_2(μ_2-S){$SC_4H(4,6-Me)_2N_2$}$_2$(μ_2-dppm)$_2$] (**2a**) and [Pd{κ-S, κ-N: $SC_4H(4,6-Me)_2N_2$}$_2$] (**2c**) complexes were recorded on a Bruker D8 Venture diffractometer using Mo-Kα radiation (λ = 0.71073 Å) as a source of X-rays along with a CCD area detector (PHOTON) with inclining phi and omega (width of 0.5 for one frame) working at a scan speed of 10 s per frame. Data acquisition as well as extraction of data was accomplished by utilizing Bruker Apex-3 and Bruker SAINT software packages using a narrow-frame algorithm (or CrysalisPro for those structures collected on the Synergy S diffractometer). The crystal structures were solved by utilizing Olex2 with the help of SHELXT [25] structure solution program by employing intrinsic phasing methods and crystal structure refinement was done with the SHELXL [26] refinement package by putting into use least squares minimization. Refinement of all non-hydrogen atoms was completed with the help of anisotropic thermal parameters. The molecular structure of complexes **1a**, **1b**, **2a** and **2c** were visualized using Mercury 2020.1.0 [27]. The crystallographic and structural determination data are given in **Table 1**.

2.2 Syntheses of complexes

2.2.1 Synthesis of [Pd{κ-S, κ-N: $SC_4H(4,6-Me)_2N_2$}{$SC_4H(4,6-Me)_2N_2$}(PPh_3)] (**1a**)

To a toluene solution (35 cm^3) of $NaSC_4H(4,6-Me)N_2$ [prepared from bis-4,6-dimethyl pyrimidin-2-yl disulfide (77.8 mg, 0.28 mmol) and sodium borohydride (21.2 mg, 0.56 mmol) in toluene-methanol], [$PdCl_2(PPh_3)_2$] (200 mg, 0.28 mmol) was added and the reaction mixtures were stirred for 4 hours at room temperature under inert condition. The solvents were evaporated under vacuum and resulted compound was washed thoroughly with diethyl ether followed by hexane to remove free phosphine. The resulting residue on extraction in toluene afforded yellow crystals of the title complex (Yield 190 mg, 73%; m.p.: 280°C (dec.)). Anal. Calcd. for $C_{30}H_{29}N_4S_2PPd$: C, 63.34; H, 4.84; N, 6.16; S, 7.05%; Found: C, 63.45;

H, 4.81; N, 6.08; S, 7.11%. UV-vis (λ_{max}): 320.4 (sh), 343 (sh) nm. ^{1}H NMR ($CDCl_3$) δ: 2.10 (s, 9H, Me), 2.15 (s, 3H, Me), 6.30 (s, 2H, $C_4\mathit{H}N_2$), 7.25-7.27 (m, 5H, Ph), 7.57-7.63 (m, 10H, Ph) ppm; $^{13}C\{^{1}H\}$: 21.45 ($-CH_3$), 22.89 ($-CH_3$), 113.88 (C-5), 127.92 (d, $^{3}J_{P\text{-}C}$ = 17.5 Hz, C-meta), 128.29 (d, $^{3}J_{P\text{-}C}$ = 20 Hz, C-meta),130.34 (t, $^{1}J_{P\text{-}C}$ = 22.5 Hz, C-ipso), 131.83 (t, $^{2}J_{P\text{-}C}$ = 33.7 Hz, C-ortho, Ph), 133.92 (C-4), 134.07 (C-4), 165.63 (C-S) ppm; $^{31}P\{^{1}H\}$ NMR ($CDCl_3$) δ: 33.7 ppm. ESI-MS m/z $[Pd\{\kappa\text{-}S, \kappa\text{-}N: SC_4H(4,6\text{-}Me)_2N_2\}\{SC_4H(4,6\text{-}Me)_2N_2\}(PPh_3)][M+2]^+$: 648.8, $[Pd\{\kappa\text{-}S, \kappa\text{-}N: SC_4H(4,6\text{-}Me)_2N_2\}(SH)][M+Na]^+$: 300.9

2.2.2 Synthesis of $[Pt\{SC_4H(4,6\text{-}Me)_2N_2\}_2(PPh_3)_2]$ (**1b**)

Prepared similarly to the above method as **1a** using bis-4,6-dimethyl pyrimidin-2-yl disulfide (52.8 mg, 0.19 mmol), sodium borohydride (14.4 mg, 0.38 mmol) and $[PtCl_2(PPh_3)_2]$ (150 mg, 0.19 mmol) to obtain pale yellow crystals of compound **1b** (Yield 144 mg, 76%; m.p.: 240°C (dec.)). Anal. Calcd. for $C_{48}H_{44}N_4S_2P_2Pt$: C, 57.71; H, 4.41; N, 5.61; S, 6.43%; Found: C, 57.69; H, 4.36; N,5.59; S, 5.98%. UV-vis (λ_{max}): 281.3 nm. ^{1}H NMR ($CDCl_3$) δ: 2.33 (s, 12H, Me), 6.38 (s, 2H, $C_4\mathit{H}N_2$), 7.10-7.25 (m, 15H, Ph) 7.62-7.76 (m, 15H, Ph); $^{31}P\{^{1}H\}$ NMR ($CDCl_3$) δ: 24.00 ppm [^{1}J(Pt-P) = 2880 Hz]. Due to poor solubility of complex **1b**, $^{13}C\{^{1}H\}$ NMR could not record with an acceptable S/N ratio. ESI-MS m/z: $[Pt\{\kappa\text{-}S, \kappa\text{-}N: SC_4H(4,6\text{-}Me)_2N_2\}\{SC_4H(4,6\text{-}Me)_2N_2\}(PPh_3)]^+$ $[M+H]^+$: 736.2, $[Pt\{SC_4H(4,6\text{-}Me)_2N_2\}(PPh_3)][M+1]^+$: 597.09, $(PPh_3)[M+1]^+$: 263.4

2.2.3 Synthesis of $[Pd_2(\mu_2\text{-}S)\{SC_4H(4,6\text{-}Me)_2N_2\}_2(\mu_2\text{-}dppm)_2]$ (**2a**)

An acetone suspension (10 cm^3) of $[PdCl_2(dppm)]$ (140 mg, 0.25 mmol) was added to a toluene-methanol solution (30 cm^3) of $NaSC_4H(4,6\text{-}Me)N_2$ [prepared from bis-4,6-dimethyl pyrimidin-2-yl disulfide (69.5 mg, 0.25 mmol) and sodium borohydride (18.9 mg, 0.50 mmol)]. The reaction contents were stirred for 7 hours at room temperature. An ensuing red solution was dried in *vacuo* to obtain brown powder which on extraction with toluene afforded red crystals of title complex (Yield 77 mg, 55%; m.p.: 140°C (dec.)). Anal. Calcd. for

$C_{62}H_{58}N_4P_4Pd_2S_3$: C, 57.6; H, 4.49; N, 4.33; S, 7.43%; Found: C, 56.8; H, 4.55; N, 4.26; S, 7.51%. UV-vis (λ_{max}): 341.1 nm. ^{1}H NMR (DMSO-d_6) δ: 1.77 (s, 2H, -C*H$_2$*), 2.51 (s, 12H, Me), 6.98 (s, 2H, $C_4\mathit{H}N_2$) 7.36-7.48 (m, 24H, Ph), 7.74-7.78 (m, 16H, Ph) ^{31}P{^{1}H} NMR (DMSO-d_6) δ: −1.99 ppm [$^1J_{P\text{-}P}$ = 99 Hz]; ^{13}C{^{1}H}: 23.23 ($-CH_3$), 24.10 ($-PCH_2$), 114.36 (C-5), 127.04 (C-meta, Ph), 127.54 (C-para, Ph) 127.94 (C-ortho, Ph), 132.73 (C-4), 163.65 (C-S), 163.86 (C-S) ppm. ESI-MS m/z $[Pd_2(\mu_2\text{-}S)\{SC_4H(4,6\text{-}Me)_2N_2\}_2(\mu_2\text{-}dppm)_2][M]^+$: 1290

2.2.4 Synthesis of [Pd{2-SC₄H(4,6-Me)₂N₂}₂(dppe)] (**2b**)

Prepared similarly to method **2a** using bis-4,6-dimethyl pyrimidin-2-yl disulfide (80 mg, 0.29 mmol), sodium borohydride (21.9 mg, 0.58 mmol) and $[PdCl_2(dppe)]$ (167 mg, 0.29 mmol) (Yield 156 mg, 69%; m.p.: 150ºC (dec.)). Anal. Calcd. for $C_{38}H_{38}N_4S_2P_2Pd$: C, 58.22; H, 4.85; N, 7.15; S, 8.19%; Found: C, 58.01; H, 4.53; N, 6.91; S, 7.99%. UV-vis (λ_{max}): 233, 290 (sh), 410 (sh) nm. ^{1}H NMR ($CDCl_3$) δ: 2.05 (s, 12H, Me), 2.41 (br, 4H, -C*H$_2$*) 6.14 (s, 2H, $C_4\mathit{H}N_2$), 7.32-7.39 (m, 10H, Ph), 7.79-7.86 (m, 10H, Ph) ppm; ^{13}C{^{1}H}: 5.43 ($-CH_3$), 23.39 ($-PCH_2$), 113.4 (C-5), 128.57 (d, $^3J_{P\text{-}C}$ = 10.5 Hz, C-meta, Ph), 131.44 (C-para, Ph), 133.71 (d, $^2J_{P\text{-}C}$ = 11.3 Hz, C-ortho, Ph), 143.46 (C-4), 152.16 (C–S) ppm; ^{31}P{^{1}H} NMR ($CDCl_3$) δ: 57.22 ppm [5]. ESI-MS m/z $[Pd\{2\text{-}SC_4H(4,6\text{-}Me)_2N_2\}_2(dppe)][M+2]^+$: 784.8, $[Pd\{\kappa\text{-}S, \kappa\text{-}N: SC_4H(4,6\text{-}Me)_2N_2\}(dppe)][M]^+$: 643.07

2.2.5 Synthesis of [Pd{κ-S, κ-N: SC₄H(4,6-Me)₂N₂}₂] (**2c**)

i) Toluene solution (10 cm^3) of $[PdCl_2(dppp)]$ (150 mg, 0.25 mmol) was added to a methanolic solution (25 cm^3) of $NaSC_4H(4,6\text{-}Me)N_2$ [prepared from bis-4,6-dimethyl pyrimidin-2-yl disulfide (69.5 mg, 0.25 mmol) and sodium borohydride (18.9 mg, 0.50 mmol)]. The reaction mixture was stirred for 4 hours and after that dried under vacuum to obtain yellow powder. The prolonged standing of the compound in dichloromethane gave yellow crystals of title complex **2c** (Yield 63 mg, 65%; m.p.: 175°C (dec.)). Anal. Calcd. for $C_{12}H_{14}N_4S_2Pd$: C, 37.42; H, 3.64; N, 14.6; S, 16.6%; Found: C, 37.54; H, 3.59; N, 14.7; S, 16.9%. ^{1}H NMR

($CDCl_3$) δ: 2.07(s, 6H, Me), 2.10 (s, 6H, Me), 6.15 (s, 2H, $C_4\mathit{H}N_2$) ppm; $^{13}C\{^1H\}$: 23.59 (-CH_3), 29.69 (-CH_3), 113.96 (C-5), 130.24 (C-4), 133.94 (C-4), 163.58 (C-S) ppm. UV-vis (λ_{max}): 307 nm. ESI-MS m/z [Pd{κ-S, κ-N: $SC_4H(4,6\text{-}Me)_2N_2\}_2$][M]$^+$: 383.97

ii) To a toluene solution (20 cm^3) of bis-4,6-dimethyl pyrimidin-2-yl disulfide (100 mg, 0.36 mmol), solution (15 cm^3) of [$Pd_2(dba)_3$] (164 mg, 0.18 mmol) was added in the same solvent and stirred the reaction mixture for 4 hours at room temperature. The solvent was evaporated under reduced pressure and the residue was extracted from dichloromethane. The aforementioned solution on slow evaporation gave yellow crystals of title compound. (Yield 54 mg, 78%; m.p.: 179°C (dec.)). Anal. Calcd. for $C_{12}H_{14}N_4S_2Pd$: C, 37.42; H, 3.64; N, 14.6; S, 16.6%; Found: C,37.45; H, 3.71; N, 15.02; S, 16.8%. UV-vis (λ_{max}): 304 nm. The ^1H NMR values are consistent with the above spectrum.

2.2.6 Synthesis of [Pd{2-SC₄H(4,6-Me)₂N₂}₂(dppp)] (2d)

To a toluene suspension of [$PdCl_2$(dppp)] (80 mg, 0.14 mmol), a dichloromethane solution of [Pb{2-$SC_4H(4,6\text{-}Me)_2N_2\}_2$] (68 mg, 0.14 mmol) was added with stirring which continued for 4 hours at toom temperature. The resulting yellow solution was concentrated to 5 cm^3 and on addition of diethyl ether (20 cm^3) a yellow precipitate was formed. The precipitate was washed with diethyl ether and dried under reduced pressure. (Yield 71 mg, 65.7%; m.p.: 210°C (dec.)). Anal. Calcd. for $C_{39}H_{40}N_4S_2P_2Pd$: C, 58.7; H, 5.02; N, 7.02; S, 8.03%; Found: C, 59.1; H, 4.59; N, 7.01; S, 8.04%. UV-vis (λ_{max}): 328.9 nm. ^1H NMR (DMSO-d_6) δ: 1.99 (br, 6H, -C*H₂*) 2.52 (s, 12 H, Me), 6.61 (s, 2H, $C_4\mathit{H}N_2$), 7.35-7.48 (m, 10H, ph), 7.53-7.79 (m, 10H, ph) ppm; $^{13}C\{^1H\}$: 19.33 (-PCH_2), 23.39 (CH_3), 27.38 (-PCH_2), 112.03(C-5), 127.59 (t, $^3J_{P\text{-}C}$ = 16.2 Hz, C-meta, Ph), 129.98 (C-para, Ph), 133.74 (t, $^2J_{P\text{-}C}$ = 16.2 Hz, C-ortho, Ph), 139.76 (C-4), 163.70 (C–S) ppm; $^{31}P\{^1H\}$ NMR (DMSO-d_6) δ: 8.55 ppm. ESI-MS m/z [Pd{2-$SC_4H(4,6\text{-}Me)_2N_2\}_2$(dppp)][M+2]$^+$:798.6, [Pd{κ-S, κ-N: $SC_4H(4,6\text{-}Me)_2N_2$(dppp)][M+1]$^+$: 658.8

2.3 Computational details

All the theoretical calculations were carried out using an *ab-initio* molecular orbital theory-based LCAO approach as implemented in the GAMESS software [28]. Geometry optimization (without any symmetry constraint) was done using the hybrid exchange correlation energy functional commonly known as B3-LYP [29, 30]. The notation B3 implies three parameters Becke exchange functional and the LYP indicates correlation functional as described by Lee-Yang-Parr. While a standard split-valence with polarization functions (6-31G(d)) was employed as a basis set [31-33] for all low-Z elements, the SBKJC [34-36] standard basis set was used for palladium.

Table 1: Crystallographic and structural determination data for [Pd{κ-S, κ-N: SC$_4$H(4,6-Me)$_2$N$_2$}{SC$_4$H(4,6-Me)$_2$N$_2$}(PPh$_3$)] (**1a**), [Pt{SC$_4$H(4,6-Me)$_2$N$_2$}$_2$(PPh$_3$)$_2$].2C$_6$H$_6$.2CH$_3$CN (**1b**), [Pd$_2$(μ-S){SC$_4$H(4,6-Me)$_2$N$_2$}$_2$(μ$_2$-dppm)$_2$] (**2a**) and [Pd{κ-S, κ-N: SC$_4$H(4,6-Me)$_2$N$_2$}$_2$] (**2c**)

Complex	[Pd{κ-S, κ-N: SC$_4$H(4,6-Me)$_2$N$_2$}{SC$_4$H(4,6-Me)$_2$N$_2$}(PPh$_3$)] (**1a**)	[Pt{SC$_4$H(4,6-Me)$_2$N$_2$}$_2$(PPh$_3$)$_2$].2C$_6$H$_6$.2CH$_3$CN (**1b**)	[Pd$_2$(μ$_2$-S){SC$_4$H(4,6-Me)$_2$N$_2$}$_2$(μ$_2$-dppm)$_2$] (**2a**)	[Pd{κ-S, κ-N: SC$_4$H(4,6-Me)$_2$N$_2$}$_2$] (**2c**)
Chemical formula	$C_{30}H_{29}N_4PPdS_2$	$C_{48}H_{44}N_4P_2PtS_2$	$C_{62}H_{58}N_4P_4Pd_2S_3$	$C_{12}H_{14}N_4PdS_2$
Formula weight	647.06	998.02	1291.98	192.03
Crystal size (mm^3)	0.246 X 0.126 X 0.071	0.321 X 0.198 X 0.125	0.359 X 0.258 X 0.126	0.100 X 0.120 X 0.150
Crystal system	triclinic	triclinic	orthorhombic	monoclinic
Space group	P-1	P-1	Fdd2	C 2/c
Unit cell dimensions				
a(Å)	11.36840(10)	10.2780(5)	53.739(3)	15.9366(15)
b(Å)	12.40250(10)	11.7410(5)	11.8862(5)	13.1635(13)
c(Å)	12.69810(10)	13.2856(7)	18.4203(8)	7.0503(7)
α(º)	92.2430(10)	92.5040(10)	90	90
β(º)	113.5620(10)	111.0060(10)	90	104.943(5)
γ(º)	112.2040(10)	112.5100(10)	90	90
Volume (Å^3)	1480.77(3)	1351.88(11)	11766.0(10)	1429.0(2)
$\rho_{calcd.}$ (g/cm^3)	1.451	1.226	1.459	1.789
Z	2	1	8	4
μ (mm^{-1})/F(000)	7.081/660	2.762/500.0	0.869/5264	5.540 /1488

Limiting indices	$-10\leq h \leq 14$	$-12\leq h \leq 12$	$-67 \leq h \leq 66$	$-18 \leq h \leq 17$
	$-15\leq h \leq 15$	$-14\leq h \leq 14$	$-14 \leq k \leq 14$	$-15 \leq k \leq 12$
	$-15\leq h \leq 15$	$-16\leq h \leq 16$	$-23 \leq l \leq 22$	$-7 \leq l \leq 8$
Θ for data collection (°)		6.72-52.874	4.67-52.878	2.04-25.00
No. of reflections collected	83545	25559	54202	3654
No. of independent reflections (R_{int})	6066(0.0461)	5503(0.0369)	6047(0.0615)	1243 (0.0288)
Data/restraints/parameters	6066/0/348	5503/0/261	6047/1/341	1243/0/90
Final R_1, wR_2 indices [$I>2\sigma I$]	0.0232, 0.0629	0.0190, 0.0544	0.0209, 0.0494	0.0338, 0.0819
R_1, wR_2 (all data)	0.0248, 0.0640	0.0190, 0.0544	0.0223, 0.0504	0.0478, 0.0916
Goodness of fit on F^2	1.059	1.086	1.036	1.041

3. Results and Discussion

Treatment of $[MCl_2(PPh_3)_2]$ (M = Pd, Pt) with two equivalents Na{2-SC_4H(4,6-Me)N_2} (freshly prepared by reductive cleavage of S-S bond of bis-4,6-dimethyl pyrimidin-2-yl disulfide with sodium borohydride) resulted compound [Pd{κ-S, κ-N: SC_4H(4,6-Me)$_2N_2$}{SC_4H(4,6-Me)$_2N_2$}(PPh_3)] (**1a**) and [Pt{SC_4H(4,6-Me)$_2N_2$}$_2$(PPh_3)$_2$] (**1b**) in quantitative good yield (**Scheme 1**).

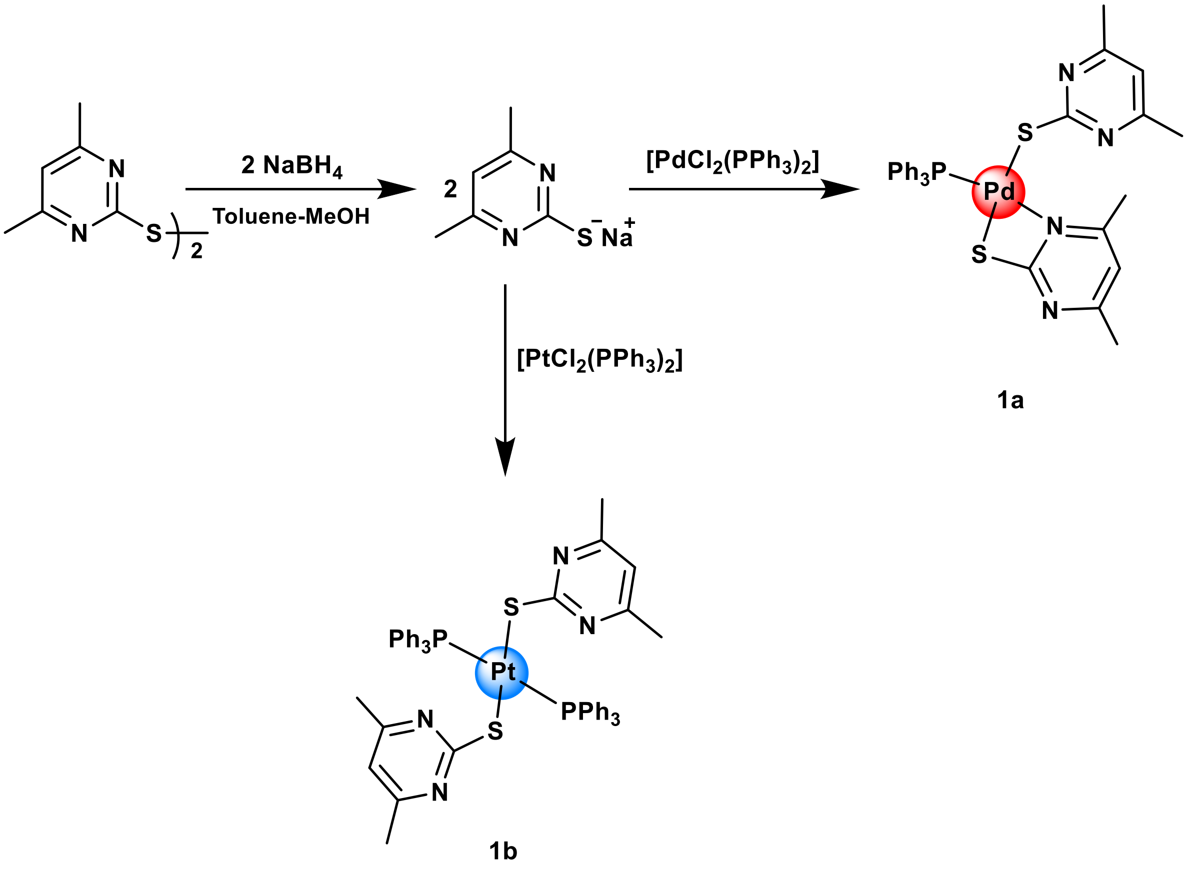

Scheme 1: Reactions of $[MCl_2(PPh_3)_2]$ (M = Pd, Pt) with sodium salt of 4,6-dimethylpyrimidine-2-thiolate

The molecular structures of complexes [Pd{κ-S, κ-N: SC_4H(4,6-Me)$_2N_2$}{SC_4H(4,6-Me)$_2N_2$}(PPh_3) (**1a**), [Pt{SC_4H(4,6-Me)$_2N_2$}$_2$(PPh_3)$_2$].$2C_6H_6$.$2CH_3CN$ (**1b**), [Pd_2(μ_2-S){SC_4H(4,6-Me)$_2N_2$}$_2$(μ_2-dppm)$_2$] (**2a**) and [Pd{κ-S, κ-N: SC_4H(4,6-Me)$_2N_2$}$_2$] (**2c**) established by X-ray diffraction analyses as shown in **Figure 3-6**. Selected interatomic parameters are summarized in **Tables 4-7**.

The crystal structure of [Pd{κ-S, κ-N: $SC_4H(4,6\text{-}Me)_2N_2$}{$SC_4H(4,6\text{-}Me)_2N_2$}($PPh_3$)] (**1a**) (**Figure 3**) revealed a distorted square planar co-ordination geometry with PNS_2 coordination core. One of the 4,6-dimethyl pyrimidine thiolate ligands is bound to the palladium in a monodentate manner while the other thiolate system has formed a four-membered chelate ring. Both Pd-S bond distances (2.3354(15) and 2.3263(5) Å) are unequal. The Pd-S1 (2.3354(15) Å) (chelated pyrimidyl thiolate) bond length is slightly elongated compared to Pd-S2 (2.3263(5) Å) (terminal thiolate). The Pd-P bond length (2.2385(5) Å) is in good conformity with the complex [Pd{κ -Se, κ-N $SeC_4H_3N_2$}$_2$ (PPh_3)] (2.2310(13) Å) [37]. The four-membered chelated ring formed by PdNCS donor atom deviated from planarity and pyrimidyl rings were perpendicular to each other. The bond length Pd-S_{avg} (2.3309 Å) is slightly elongated compared to another reported complex [Pd(tdt)$(PPh_3)_2.C_2H_4Cl_2$] (tdt = 1,2-toluenedithiolate) (2.3166(6)/2.283(6) Å). The Pd-N bond distance (2.1567(16) Å) is slightly longer than that in [PdCl(Spy)(PPh_3)] (2.112(13) Å).

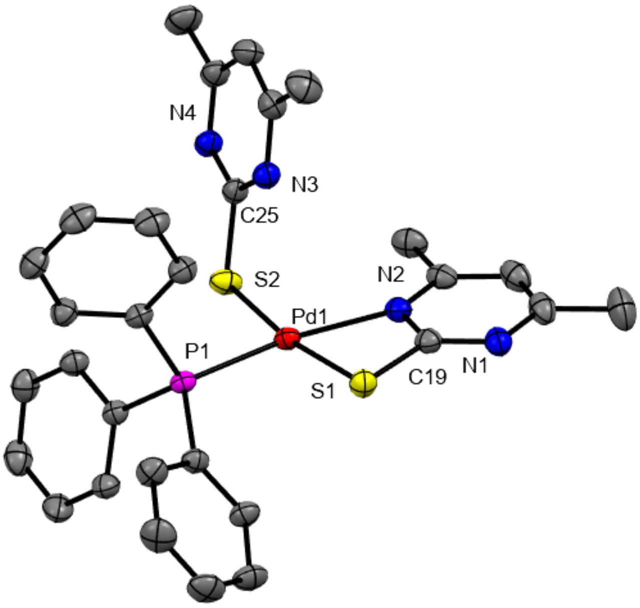

Figure 3: ORTEP diagram of [Pd{κ-S, κ-N: $SC_4H(4,6\text{-}Me)_2N_2$}{$SC_4H(4,6\text{-}Me)_2N_2$}($PPh_3$)] (**1a**) with atomic number scheme. The ellipsoids were drawn at the 50% probability level.

The $^{31}P\{^{1}H\}$ NMR of complex **1a** exhibited a single resonance at 33.7 ppm which is deshielded compared to the reported *trans* complex $[Pd(SAr)_2(PPh_3)_2]$ (Ar = py, pym, ph) [38, 39] [**Table 2**]. It suggests that an appearance of the signal is aroused due to the phosphorus *trans* to pyridyl nitrogen atom.

Table 2: Comparative prospects of chemical shift along with coupling constants

Complex	δ(ppm)	$^{1}J_{Pt-P}$ (Hz)	Reference
$[Pd(SC_5H_4N)_2(PPh_3)_2]$	25.9	-	27
$[Pd(SC_4H_3N_2)_2(PPh_3)_2]$	26.0	-	27
$[Pt(SC_5H_4N)_2(PPh_3)_2]$	24.4	2845	15
$[Pt\{\kappa\text{-}S, \kappa\text{-}N: SC_5H_4N\}\{SC_5H_4N_2\}(PPh_3)\}]$	7.7	3846	15
$[Pt(SeC_4H_3N_2)_2(PPh_3)_2]$	20.3	2792	37
$[Pt\{\kappa\text{-}Se' \kappa\text{-}N: SeC_4H_3N_2\}\{SeC_4H_3N_2\}(PPh_3)\}]$	7.4	3873	37
$[Pt\{SC_4H(4,6\text{-}Me)_2N_2\}_2(PPh_3)_2]$	24.00	2880	current work
$[Pt\{\kappa\text{-}S, \kappa\text{-}N: SC_4H(4,6\text{-}Me)_2N_2\}\{SC_4H(4,6\text{-}Me)_2N_2\}(PPh_3)$	6.09	4126	current work

Complex $[Pt\{SC_4H(4,6\text{-}Me)_2N_2\}_2(PPh_3)_2].2C_6H_6.2CH_3CN$ (**1b**) (**Figure 4**) is a centrosymmetric monomer in which the two triphenyl phosphine molecules are connected to the platinum center through phosphorus atom in *trans* position. However, remaining sites of the platinum are occupied by 4,6-dimethyl pyrimidine-2-thiol ligands that showed *anti*-configuration and coplanar (interplanar angle = 0.0^{o}) nature. The closest centroid-centroid distance between phenyl ring of PPh_3 and pyrimidyl ring is 3.515 Å leads to π-π interaction. Metal centre had adopted distorted square planar geometry with Pt-S bond distance (2.3373(5) Å) similar to complex *trans* $[Pt(S\text{-}C_4H_3SN_2)_2(PPh_2Me)_2]$ (2.3380(12) Å) [19] whereas shorter with respect to complex $[Pd\{2\text{-}SC_4H(4,6\text{-}Me)_2N_2\{SC(NH_2)_2\}]Cl$ (Pd-S1 = 2.376 (8) and Pd-S2 = 2.361 (7) Å) [5]. The Pt-P bond lengths (2.3217(5) Å) are in good agreements to reported complexes $[Pt(SePh)_2(PEt_3)_2]$, $[Pt(SeTh)_2(PPh_3)_2]$, $[Pt(SeC_4H_3N_2)_2(PPh_3)_2].2CH_2Cl_2$ (2.312(2)), 2.3204(16) and (2.3128(19) Å) [37, 40, 41]. The two acute angles P1-Pt1-S1(85.966(19)º) and two obtuse angles S1-Pt1-P1 (94.034(19)º) are comparable to the documented compound *trans*-$[Pt(Spy)_2(PPh_3)_2]$ (Spy = C_5H_4NS) [42].

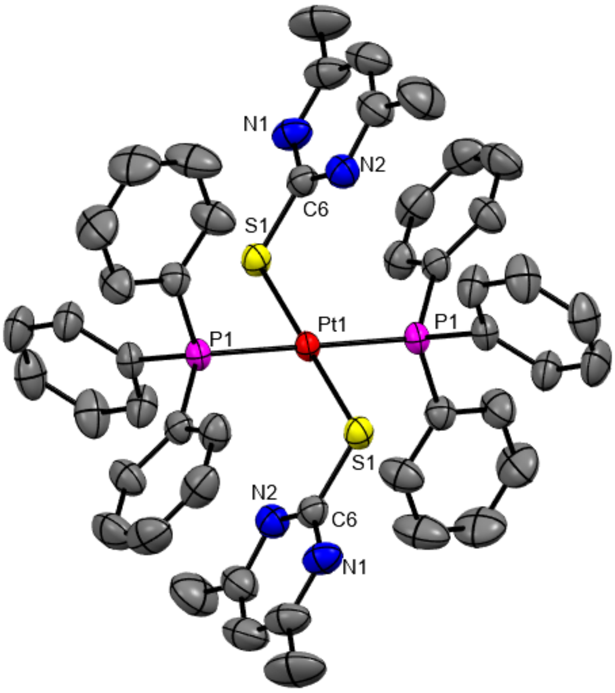

Figure 4: ORTEP diagram of $[Pt\{SC_4H(4,6\text{-}Me)_2N_2\}_2(PPh_3)_2].2C_6H_6.2CH_3CN$ (**1b**) with atomic number scheme. The ellipsoids were drawn at the 50% probability level.

The $^{31}P\{^1H\}$ NMR spectrum of complex $[Pt\{SC_4H(4,6\text{-}Me)_2N\}_2(PPh_3)_2]$ (**1b**) indicates the existence of two moieties in solution by showing two different signals at 24 ppm and 6.09 ppm with their respective satellites. The resonance at 24 ppm having $^{195}Pt\text{-}^{31}P$ coupling constant 2880 Hz corresponds to the existence of *trans* product $[Pt\{SC_4H(4,6\text{-}Me)_2N_2\}_2(PPh_3)_2]$ whereas presence of shielded resonance at 6.09 ppm with $^{195}Pt\text{-}^{31}P$ coupling constant 4126 Hz corroborated to $[Pt\{\kappa\text{-}S, \kappa\text{-}N: SC_4H(4,6\text{-}Me)_2N_2\}\{SC_4H(4,6\text{-}Me)_2N_2\}(PPh_3)]$ in which one of the 4,6-dimethyl pyrimidine-2-thiolate ligands get coordinated through sulphur and pyrimidyl nitrogen which consequently knocked out PPh_3 in phosphine oxide form (**Figure 2, Scheme 2**). Several attempts have been implemented to separate the former chelated species but could not obtain pure product. The magnitude of $^{1}J_{Pt\text{-}P}$ reveals the presence of *trans* configuration of complex **1b** and is in good agreement with the reported value [15]. The quite shielded and higher coupling constant supports the formation of chelated species in *in-situ*. Similar observations were previously reported by us, during the reaction of $(SeC_4H_3N_2)_2$ with $[Pt(PPh_3)_4]$ that resulted in products $[Pt(SeC_4H_3N_2)_2(PPh_3)_2]$ and $[Pt\{\kappa^2\text{-}SeC_4H_3N_2\}\{SeC_4H_3N_2\}(PPh_3)\}]$ displaying resonances at 7.4 and 20.3 ppm with coupling constants $^{1}J_{Pt\text{-}P}$ is 2792 and 3873 Hz respectively [37].

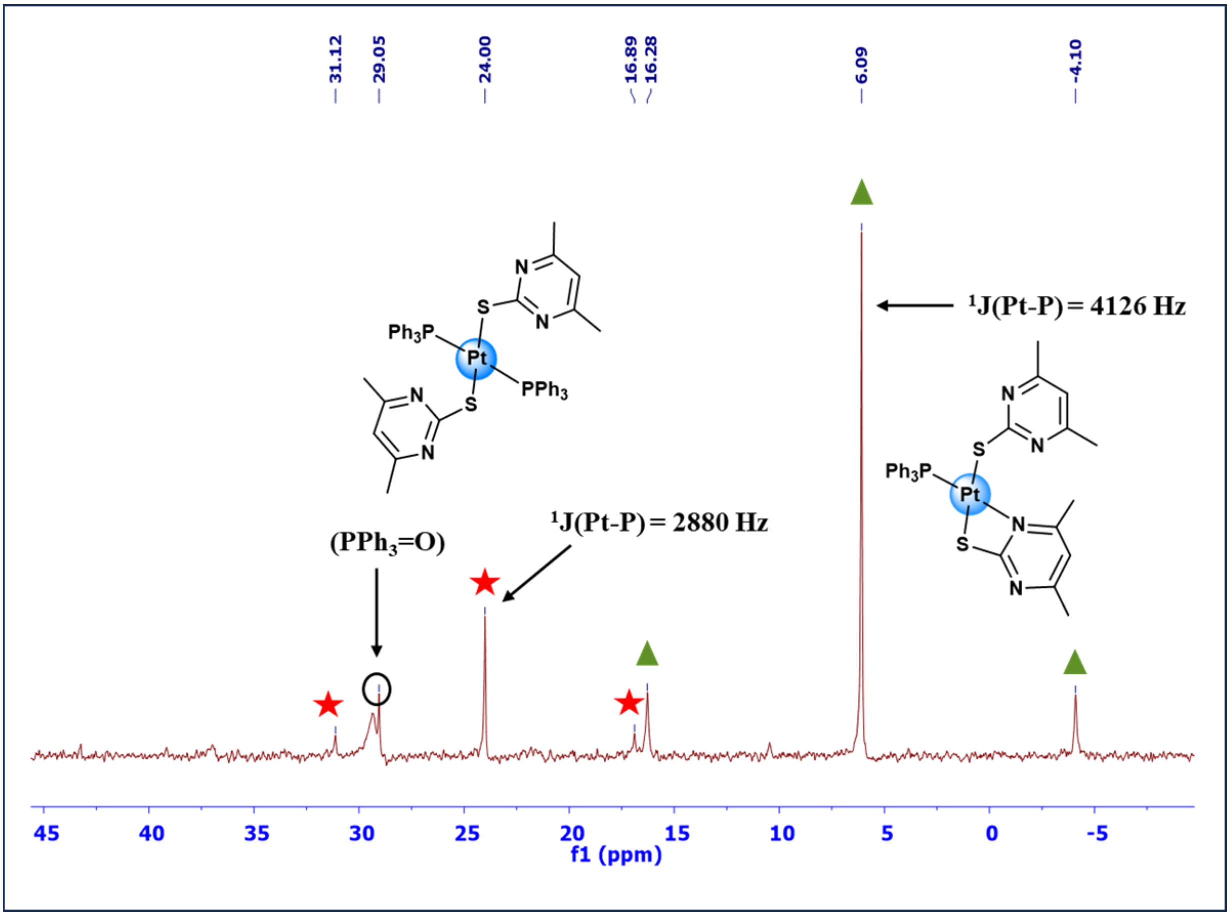

Figure 2: $^{31}P\{^{1}H\}$ NMR spectrum of $[Pt\{SC_4H(4,6\text{-}Me)_2N_2\}_2(PPh_3)_2]$ (**1b**) (represented through red stars) and $[Pt\{\kappa\text{-}S, \kappa\text{-}N: SC_4H(4,6\text{-}Me)_2N_2\}\{SC_4H(4,6\text{-}Me)_2N_2\}(PPh_3)]$ (represented through green triangles)

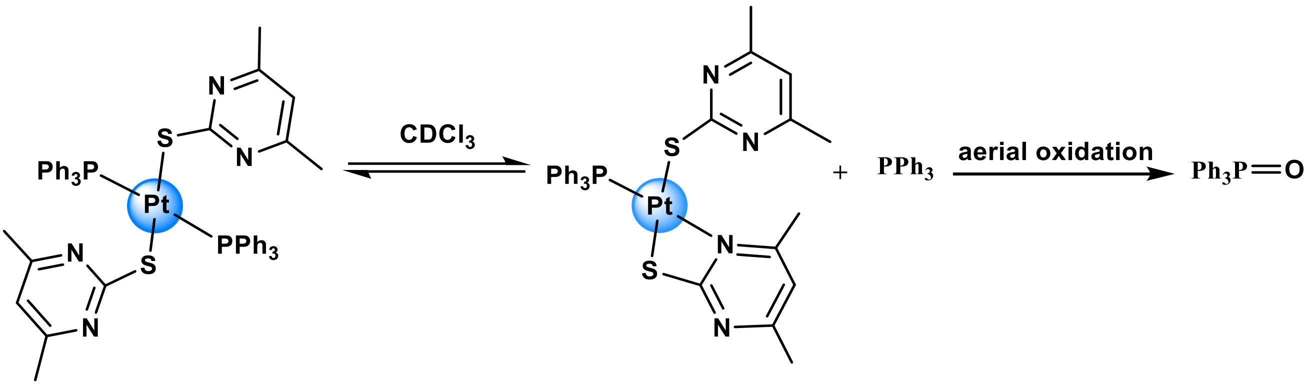

Scheme 2: Equilibrium between $[Pt\{SC_4H(4,6\text{-}Me)_2N_2\}_2(PPh_3)_2]$ (**1b**) and $[Pt\{\kappa\text{-}S, \kappa\text{-}N{:}\ SC_4H(4,6\text{-}Me)_2N_2\}\{SC_4H(4,6\text{-}Me)_2N_2\}(PPh_3)$

Similar reactions with chelated phosphine precursors $[PdCl_2(P\text{-}P)]$ (P-P = dppm, dppe, dppp) afforded various products depending upon the nature of phosphine [**Table 3**]. The reaction of $[PdCl_2(dppm)]$ with two mole of $Na\{2\text{-}SC_4H(4,6\text{-}Me)_2N_2\}$ resulted a red crystalline solid of complex $[Pd_2(\mu_2\text{-}S)\{SC_4H(4,6\text{-}Me_2)_2N_2\}_2(\mu_2\text{-}dppm)_2]$ (**2a**). An important observation has been noted in complex **2a** that the nature of "dppm ligand" has transformed to bridging mode and cleavage of S-C bond of Spym to afford S^{2-} as pendant which is flanked between two palladium centres. Hence, the bridging behaviour of 'dppm' and sulphide moiety provided extra stability to afford a dimeric complex **2a**. Another important observation correlated with simultaneous cleavage of S-S and S-C bonds. It is worth mentioning here that the reaction of $[PdCl_2(dppm)]$ with pyridine thiolate afforded mixed valent dimeric complex of composition $[Pd_2(\mu_2\text{-}Spy)_3(\mu_2\text{-}dppm)]Cl$ [36]. A similar reaction with higher congeners of the chalcogen family yielded tetranuclear complex $[Pd_4(\mu_2\text{-}Te)(\mu_2\text{-}Tepy)(Tepy)(\mu\text{-}dppm)_2]$ [14]. A centrosymmetric dimeric complex $[Pd_2(\mu_2\text{-}S)\{SC_4H(4,6\text{-}Me)_2N_2\}_2(\mu_2\text{-}dppm)_2]$ (**2a**) (**Figure 5**) crystallized in the orthorhombic space group Fdd2. The coordination core of each palladium atom in complex **2a** is defined by bridging dppm and 4,6-dimethyl pyrimidyl thiolate ligands in which pyrimidyl rings are in *anti*-configuration. Both palladium centres are interconnected through a bridged sulphide which lay above the plane and equidistant position from both palladium atoms. Also, the $S_{2terminal}Pd_2S_{bridge}$ plane is nearly perpendicular to the Pd-P vectors.

The side view of molecular structure **2a** represents the presence of both twisted fused rings that have acquired half-chair conformation and one of the methylene groups lies above Pd-S-Pd bond. The bond length of Pd-S$_{\text{terminal}}$ (2.3601(13) Å) is longer than Pd-S$_{\text{bridge}}$ (2.3278(11) Å) which is due to the strong *trans* effect of bridging sulphides as compared to aryl thiolates. The Pd-S bond distances (2.3601(13) and 2.3278(11) Å) are similar to complex [Pd$_2$(μ_2-S,N-C$_5$H$_4$SN)$_3$(μ_2-dppm)]Cl (Pd1-S2 = 2.296(2); Pd2-S1 = 2.305(3); Pd2-S3 = 2.355(3) Å) [43] but shorter than the complex of higher congener [Pd(SeC$_5$H$_3$(3-CONHPh)N)$_2$(PPh$_3$)] (Pd-Se = 2.441 (9) Å) [44]. The Pd1-P1 (2.3150(10) Å) bond length is slightly elongated compared to Pd-P2 (2.2916(10) Å) but well in range with the reported complexes [M$_2$(μ-κ^2: N,S-pyS)$_3$(μ-P,P-dppm)]Cl (M = Pd, Pt) [45]. An increment was observed in the distance between two palladium centres (3.228 Å) due to the insertion of S atom which is in accordance with the earlier reported complex [Pd$_2$(dppm)$_2$(μ-S)Cl$_2$] (3.258(2) Å [46]. The Pd-S-Pd (87.80(5)°) bond angle is greater than Pd-Se-Pd (78.4°) in [Pd$_2$Cl$_2$(μ-Se)(dppmMe)$_2$] [47]. The diagonal angle S-Pd-S (177.42(5)°) deviated from linear fashion as compared to documented values [48].

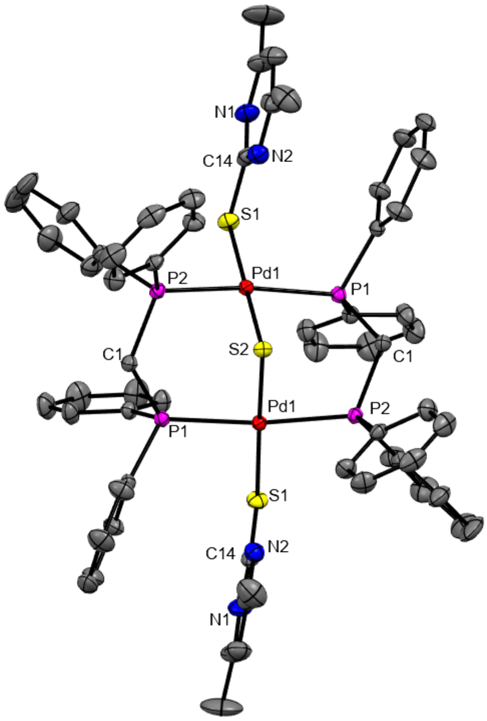

A

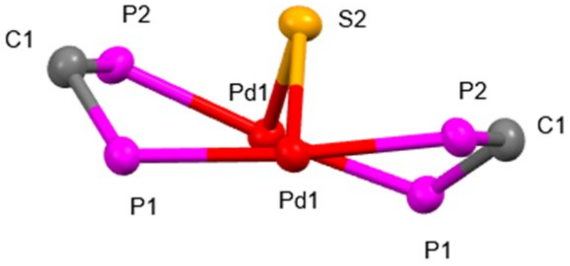

B

Figure 5: (**A**) ORTEP diagram of $[Pd_2(\mu_2\text{-}S)\{SC_4H(4,6\text{-}Me)_2N_2\}_2(\mu_2\text{-dppm})_2]$ (**2a**) with atomic number scheme. The ellipsoids were drawn at the 50% probability level. (**B**) Side view showing conformations of the rings.

The $^{31}P\{^1H\}$ NMR of complex $[Pd_2(\mu_2\text{-}S)\{SC_4H(4,6\text{-}Me_2)_2N_2\}_2(\mu_2\text{-dppm})_2]$ (**2a**) displayed double centred resonance at $\delta = -1.99$ ppm against magnetically inequivalent phosphorus atoms. Similar non-equivalency was reported in case of $[Pd_4(\mu_2\text{-}Te)(\mu_2\text{-}Tepy)(Tepy)(\mu\text{-dppm})_2]$ [14]. ESI-MS spectrum of complex **2a** displayed a prominent signal at m/z ratio of 644.9 which supports asymmetric fragmentation of dimeric species through bridging sulphide atom. Most probably, two asymmetric fragments of "$[Pd(SC_4H(4,6\text{-}Me_2)_2N_2\}(dppm)]$" in solution form bridged through sulphide during the course of reaction to result complex $[Pd_2(\mu_2\text{-}S)\{SC_4H(4,6\text{-}Me_2)_2N_2\}_2(\mu_2\text{-dppm})_2]$. The reactivity of $[PdCl_2(dppe)]$ is straight and results the formation of *cis*-configured monomeric complex $[Pd\{2\text{-}SC_4H(4,6\text{-}Me_2)_2N_2\}_2(dppe)]$ (**2b**). A single resonance at 57.22 ppm was obtained in $^{31}P\{^1H\}$ NMR of compound **2b** which is shielded compared to $[Pd(SC_5H_4N)_2(dppe)]$ ($\delta = 59.5$ ppm) [20] and well matched with the reported value [20]. The shielding prospect of signal in complex **2b** is encountered due to the presence of extra electronegative nitrogen in pyrimidyl ring compared to pyridyl (**Scheme 3**).

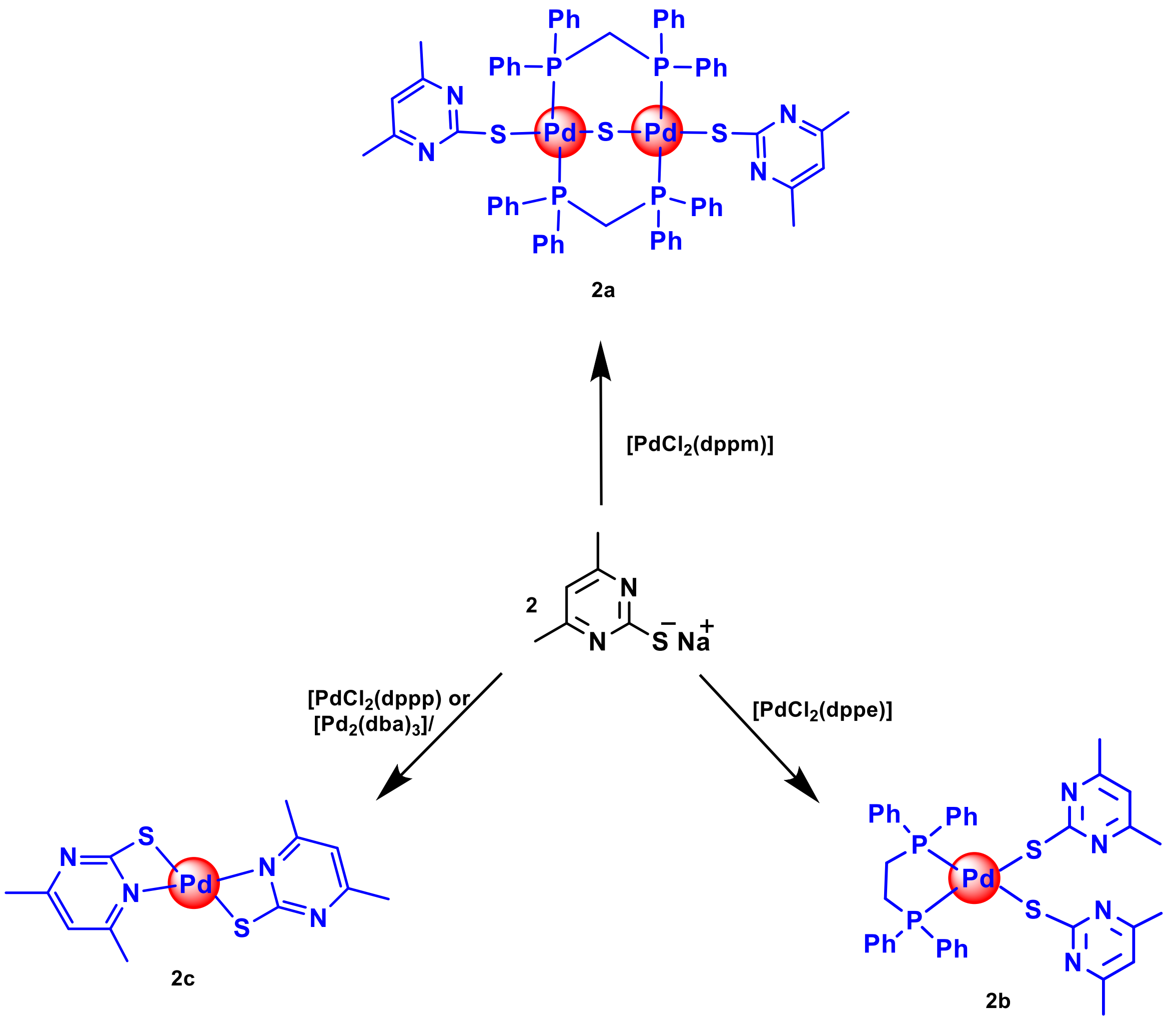

Scheme 3: Reactions of [PdCl$_2$(P-P)$_2$] [(P-P)$_2$ = dppm, dppe, dppp) and [Pd$_2$(dba)$_3$] with sodium salt of 4,6-dimethylpyrimidine-2-thiolate

Table 3: Comparative reactivity of various N-heterocyclic thiolate ligand systems

Palladium precursors	**Ligands**	**Complexes**	**References**
[PdCl$_2$(dppm)]	PyS$^-$	1.[Pd(dppm)(SC$_5$H$_4$N)$_2$]	17
		2.[Pd$_2$(μ- κ^2:N,S-pyS)$_3$(μ-P,P-dppm)]Cl	45
	PymS$^-$	[Pd(dppm)(SC$_4$H$_3$N$_2$)$_2$]	51
	4,6-Me$_2$PymS$^-$	[Pd$_2$(μ$_2$-S){SC$_4$H(4,6-Me$_2$)$_2$N$_2$}$_2$(μ$_2$-dppm)$_2$]	current work
[PdCl$_2$(dppe)]	PyS$^-$	[Pd(dppe)(SC$_5$H$_4$N)$_2$]	17

	$PymS^-$	$[Pd(dppe)(SC_4H_3N_2)_2]$	51
	$4,6\text{-}Me_2PymS^-$	$[Pd\{2\text{-}SC_4H(4,6\text{-}Me_2)_2N_2\}_2(dppe)]$	current work
$[[PdCl_2(dppp)]$	PyS^-	$[Pd(dppp)(SC_5H_4N)_2]$	17
	$PymS^-$	–	–
	$4,6\text{-}Me_2PymS^-$	$[Pd\{\kappa\text{-}S, \kappa\text{-}N{:}\ SC_4H(4,6\text{-}Me)_2N_2\}_2]$	current work

The outcome of the reaction between "$[PdCl_2(dppp)]$" with pyrimidine thiolate analogues is remarkedly different from the rest of the chelating phosphine precursor. In this case, differing to our expectation, complex $[Pd\{\kappa\ \text{-}S, \kappa\text{-}N{:}\ SC_4H(4,6\text{-}Me)_2N_2\}_2]$ (**2c**) was isolated by the reaction between $[PdCl_2(dppp)]$ with two equivalent of sodium salt of bis-4,6-dimethyl pyrimidyl disulfides. The latter complex was also synthesized through an oxidative addition reaction between $[Pd_2(dba)_3]$ with $\{SC_4H(4,6\text{-}Me_2)_2N_2\}_2$. The molecular structure of compound $[Pd\{\kappa\text{-}S, \kappa\text{-}N{:}\ SC_4H(4,6\text{-}Me)_2N_2\}_2]$ (**2c**) (**Figure 6**) crystallizes as discrete monomers in the monoclinic space group C 2/c. The palladium is surrounded by two nitrogen and sulphur atoms of 4,6-dimethylpyrimidine-2-thiolate ligands *trans* to each other. The palladium centre is situated on the crystallographic centre of symmetry in which both the Pd-N bond lengths are exactly same i.e., 2.013(3) Å and Pd-S (2.3424(11)) bond distance which is similar to the complex *trans*-$[Pd(PPh_3)_2(Spy)_2]$(py = pyridine) [38], $[Pd(\kappa\text{-}S\text{-}imzSH)_4]Cl_2\cdot 2H_2O$ (2.3305 (4), 2.3333 (4) Å) [45] and $[Pd(Imt)_2(PPh_3)_2].3.5H_2O$ (Imt = imidazolidine-2-thione) (2.3397(13), 2.3249(13) Å) [49]. The angles between N-Pd-N and S-Pd-S are exactly 180º. However, the bond angle N1-Pd1-S1 (70.20(10))º is acute due to the formation of four membered chelate ring whereas the angle between S1-Pd1-N1i is 109.80(10)º.

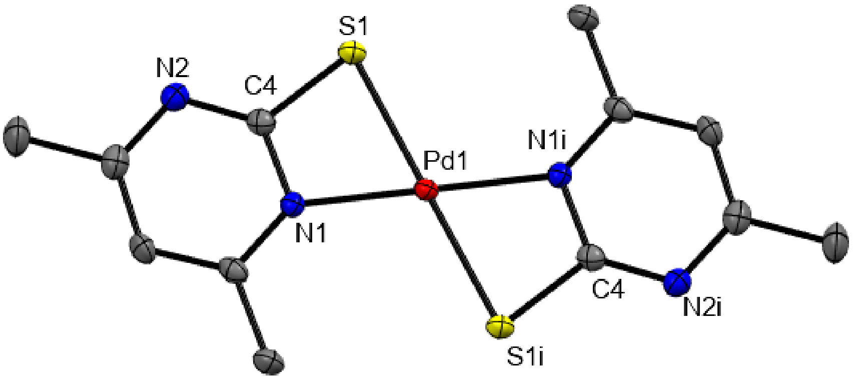

Figure 6: ORTEP diagram of $[Pd\{\kappa\text{-}S, \kappa\text{-}N: SC_4H(4,6\text{-}Me)_2N_2\}_2]$ (**2c**) with atomic number scheme. The ellipsoids were drawn at the 50% probability level.

The $^{31}P\{^1H\}$ NMR displayed silent behaviour supporting the removal of "dppp" ancillary ligand. ^1H NMR displayed all possible peak multiplicities in complex **2c**. Lobana and coworkers reported the reaction of $[PdCl_2(dppp)]$ with pyridine thiolates in the presence of NaOH resulted in monomeric product $[Pd(SC_5H_4N)_2(dppp)]$. In order to examine the reactivity rate between sodium salt and lead salt of 4,6-dimethyl pyrimidine thiol, the reaction between $[PdCl_2(dppp)]$ with two equivalents of $[Pb(2\text{-}SC_4H(4,6\text{-}Me)_2N_2]$ was carried out which yielded an expected mononuclear complex $[Pd\{2\text{-}SC_4H(4,6\text{-}Me)_2N_2\}_2(dppp)]$ (**2d**) (**Scheme 4**). The chemical shift at 8.55 ppm in $^{31}P\{^1H\}$ NMR of complex **2d** is very close to analogues complexes $[Pd(2\text{-}SC_5H_4N)_2(dppp)]$ [20]. It seems that the reaction on carrying through sodium salt is rapid and as consequences cleaved off the "dppp" moiety whereas the reaction through lead salt is sluggish and yielded expected mononuclear product.

The electronic shift of the complexes $[Pd\{\kappa\text{-}S, \kappa\text{-}N: SC_4H(4,6\text{-}Me)_2N_2\}\{SC_4H(4,6\text{-}Me)_2N_2\}(PPh_3)]$ (**1a**), $[Pt\{SC_4H(4,6\text{-}Me)_2N_2\}_2(PPh_3)_2]$ (**1b**), $[Pd_2(\mu_2\text{-}S)\{SC_4H(4,6\text{-}Me)_2N_2\}_2(\mu_2\text{-}dppm)_2]$ (**2a**), $[Pd\{\kappa\text{-}S, \kappa\text{-}N: SC_4H(4,6\text{-}Me)_2N_2\}_2]$ (**2c**) and $[Pd\{2\text{-}SC_4H(4,6\text{-}Me)_2N_2\}_2(dppp)]$ (**2d**) have shown absorption bands in the region of 281-341 nm which are attributed to bathochromic shift with respect to bis-4,6-dimethyl pyrimidin-2-yl disulfide. A similar type of observation has been mentioned in the literature [50].

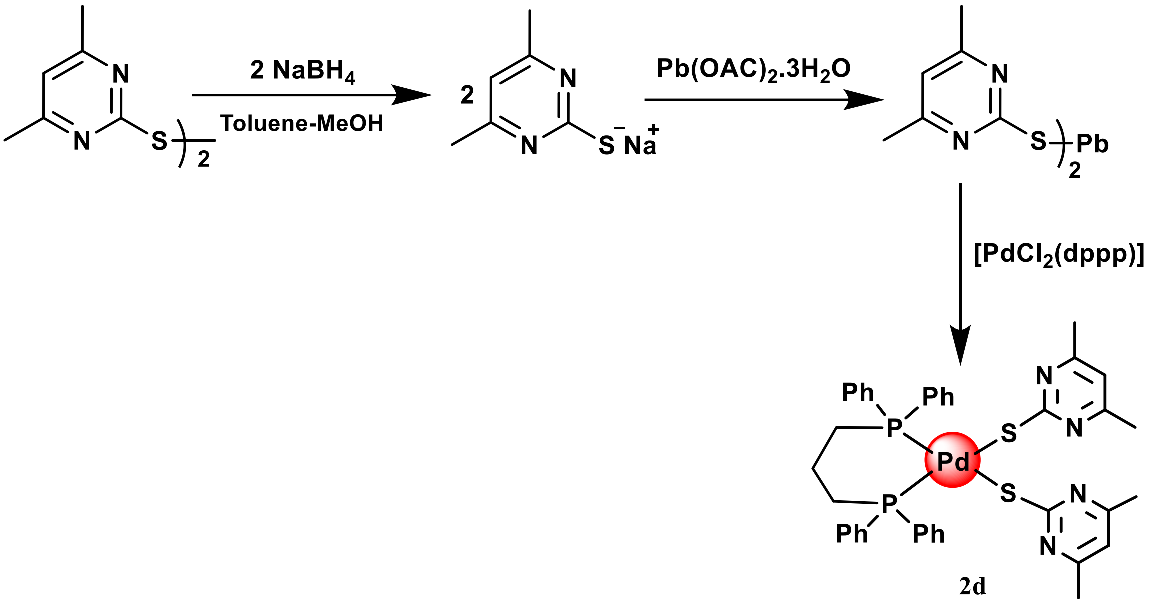

Scheme 4: Reactions of [PdCl$_2$(dppp)$_2$] with lead-2-pyrimidyl(4,6-Me)$_2$thiolate

Table 4: Selected bond lengths (Å) and bond angles (º) for [Pd{κ-S, κ-N: SC$_4$H(4,6-Me)$_2$N$_2$}{SC$_4$H(4,6-Me)$_2$N$_2$}(PPh$_3$)] (**1a**)

Pd1-P1	2.2385(5)	Pd1-N2	2.1567(16)
Pd1-S1	2.3354(15)	Pd1-S2	2.3263(5)
S2-C25	1.747(2)	S1-C19	1.741(2)
P1-Pd1-S2	90.699 (18)	S1-Pd1-N2	69.48(5)
P1-Pd1-S1	97.414(17)	S2-Pd1-N2	102.43(5)
S1-Pd1-S2	171.392 (19)	P1-Pd1-N2	166.87(5)
Pd1-S2-C25	100.96(6)	Pd1-S1-C19	81.48(7)

Table 5: Selected bond lengths (Å) and bond angles (º) for [Pt{SC$_4$H(4,6-Me)$_2$N$_2$}$_2$(PPh$_3$)$_2$] (**1b**)

Pt1-P1	2.3217(5)	Pt1-S1	2.3373(5)
C6-N1	1.344(3)	C6-N2	1.335(3)

S1-C6	1.749(2)		
P1-Pt1-S1	85.966(19)	S1-Pt1-P1	94.034(19)
N1-C6-S1	113.34(19)	Pt1-S1-C6	108.48(8)
P1-Pt1-P1	180.0(3)	S1-Pt1-S1	180.0(17)

Table 6: Selected bond lengths (Å) and bond angles (°) for [Pd$_2$(μ-S){SC$_4$H(4,6-Me)$_2$N$_2$}$_2$(μ-dppm)$_2$] (**2a**)

Pd1-P1	2.3150(10)	Pd1-P2	2.2916(10)
Pd1-S1	2.3601(13)	Pd1-S2	2.3278(11)
S1-C14	1.741(4)		
P1-Pd1-S1	89.10(4)	P2-Pd1-S2	80.17(3)
S1-Pd1-P2	98.87(5)	S2-Pd1-P1	91.91(4)
S1-Pd1-S2	177.42(5)	P1-Pd-P2	171.96(6)
Pd1-S2-Pd1	87.80(5)		

Table 7: Selected bond lengths (Å) and bond angles (°) for [Pd{κ-S, κ-N: SC$_4$H(4,6-Me)$_2$N$_2$}$_2$] (**2c**)

Pd1-N1	2.013(3)	Pd1-S1	2.3424(11)
S1-C4	1.745(5)	C4-N2	1.325(6)
N1-Pd1-S1	70.20(10)	N1-C4-S1	108.7(3)
N1-Pd1-N1i	180.0	S1-Pd1-S1i	180.0
S1-Pd1-N1i	109.80(10)		

4. Computational studies

The substitution reaction of [PdCl$_2$(P-P)] (P-P = PPh$_3$, dppe, dppm, dppp) with 4,6-dimethylpyrimidine-2-thiol gives different products i.e., dimeric, monomeric and chelated complexes etc. In order to rationalize this observation theoretical calculations were carried out under DFT formalism. The aim of the calculation is to compare the geometrical and electronic structure of [PdCl$_2$(P-P)] (P-P = PPh$_3$, dppe, dppm, dppp) and correlate these features with observed variation in their substitution reaction with sodium salt of 4,6-dimethyl pyrimidin-2-thiol. **Figure-7** shows the optimized geometry of [PdCl$_2$(P-P)] (P-P = PPh$_3$, dppe, dppm, dppp).

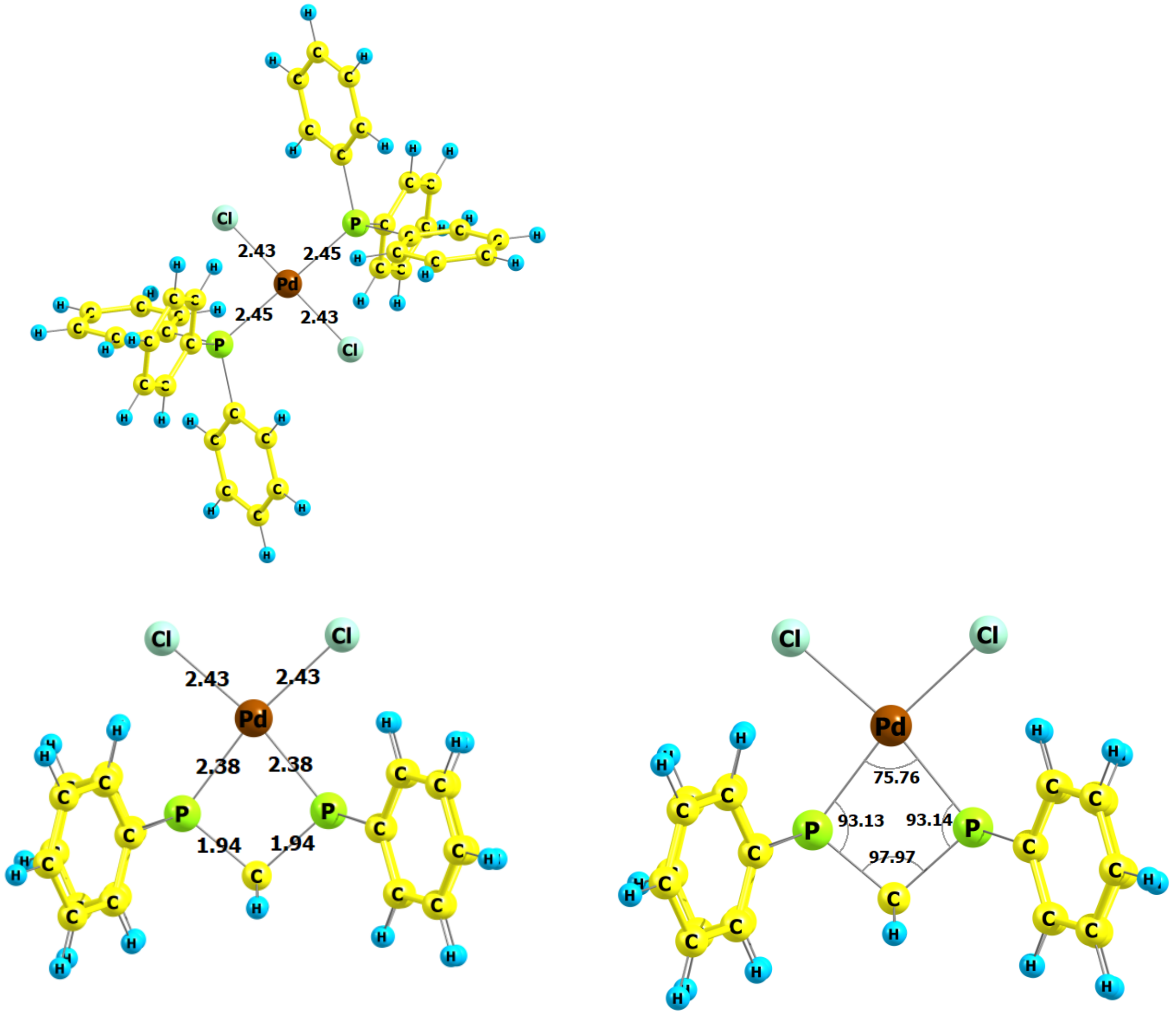

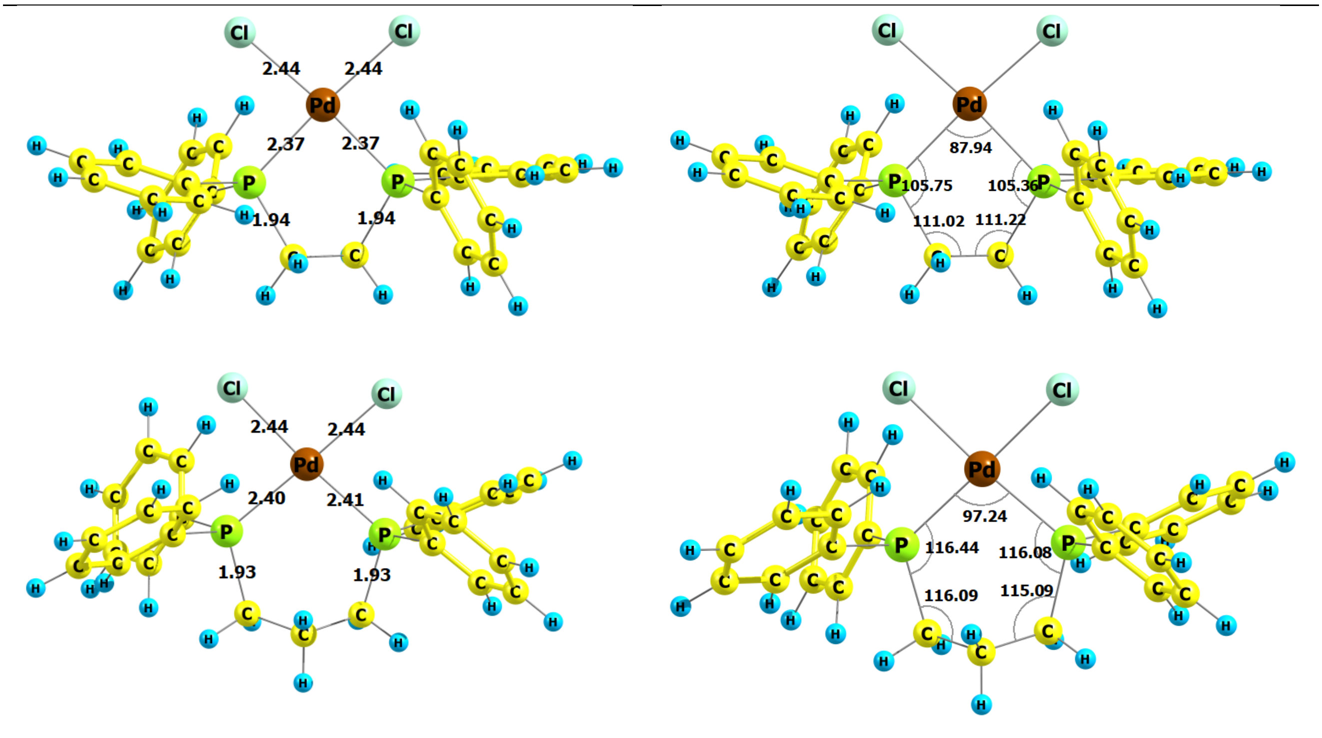

Figure 7: Optimized Geometry of metal precursors $[PdCl_2(P\text{-}P)]$ (P-P = PPh_3, dppm, dppe, dppp)

It is clear from **Figure-7** that the structure of $[PdCl_2(P\text{-}P)]$ (P-P = PPh_3, dppm, dppe, dppp) varies with chelating phosphine (P-P) ligands. Specially two contrasting variations are observed (i) the P-Pd-P angle got significant changes for chelating phosphine ligands as it got opened systematically. (ii) The dihedral angle between the aryl rings is quite different. These structure differences force Pd(ligand)$_4$ moiety to drift away from the core square planar structure requiring P-Pd-P angle to be around 90^o. While for dppm, the aryl rings are eclipsed towards each other, the P-Pd-P is quite far from the right angle, contrary for dppe the aryl rings got pseudo staggered with respect to each other, but the P-Pd-P angle is quite close to 90^o. For dppp, the P-Pd-P angle is again moved far from 90^o and inches closer to 100^o. These geometrical changes also influence their electronic structure. The frontier molecular orbitals (FMOs) of $[PdCl_2(P\text{-}P)]$ (P-P = PPh_3, dppm, dppe, dppp) are presented in **Figure 8**. In the two upper Highest Occupied Molecular Orbital (HOMOs) of $[PdCl_2(P\text{-}P)]$ one has an antibonding combination of Pd atom`s *d*-orbitals and *p*-orbitals of chloride ions and the other has bonding combination of atomic orbital of Pd and P. The extent of relative overlap between Pd and P atomic orbital was less for dppp probably owing to larger value of P-Pd-P. The relative ordering of these two varies for P-P = dppm, dppe, dppp. For dppe, the frontier molecular orbitals having a bonding combination of Pd and P becomes HOMO. Irrespective of ligand, palladium contributes in the frontier molecular orbitals indicating the metal orbital will have an important role in the reactivity of complex. However, the Lowest Unoccupied Molecular Orbital (LUMO) of [PdCl$_2$(P-P)] almost remains unaffected by varying the chelating phosphine (P-P) ligands. LUMO is localized on the chlorine and phosphorus atom and additionally does have contribution from the central palladium atom. The higher unoccupied orbital (LUMO+1) marginally gets affected by varying chelating phosphines (P-P). (LUMO+1) orbital is localized on the aryl ring and has very small or negligible contribution from the central palladium atom. The contribution from aryl has been more prominent for dppm in comparison to dppe and dppp probably owing to a greater extent of symmetry in the molecular structure.

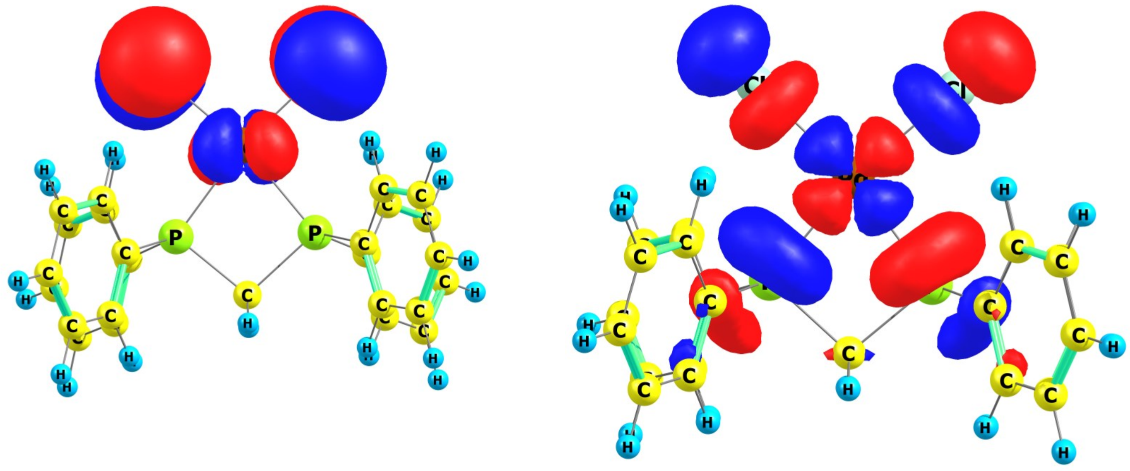

[PdCl$_2$(dppm)]: HOMO **[PdCl$_2$(dppm)]: LUMO**

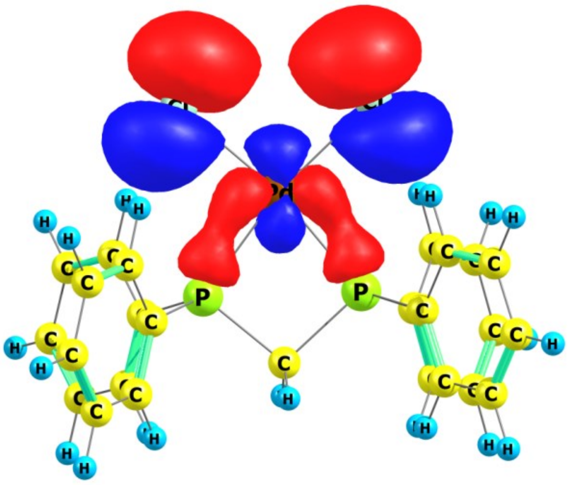

[PdCl$_2$(dppm)]: HOMO-1

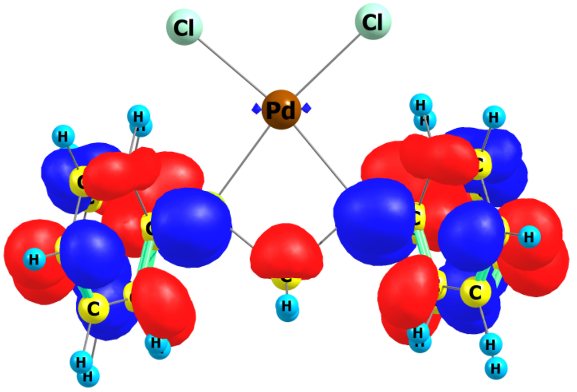

[PdCl$_2$(dppm)]: LUMO+1

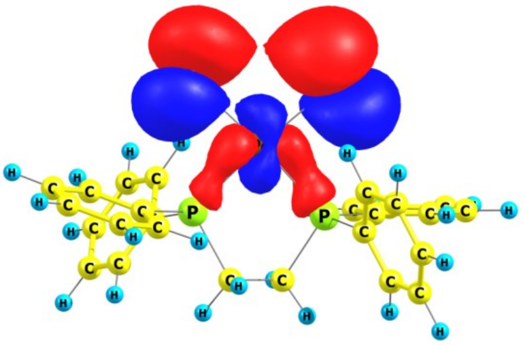

[PdCl$_2$(dppe)]: HOMO

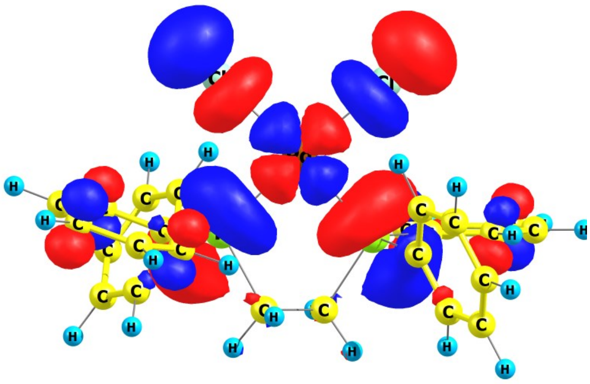

[PdCl$_2$(dppe)]: LUMO

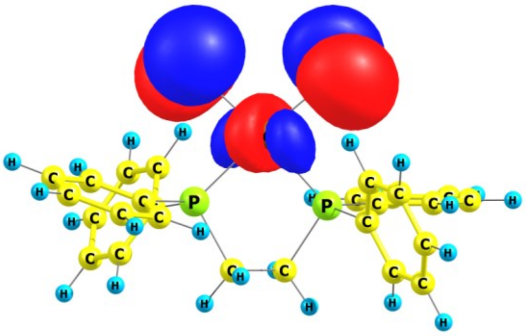

[PdCl$_2$(dppe)]: HOMO-1

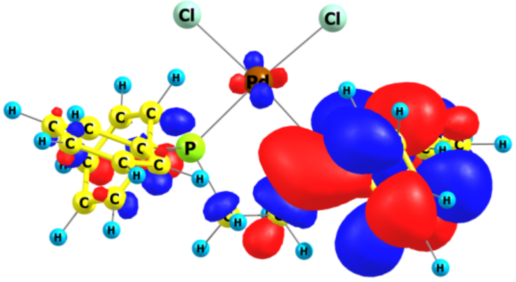

[PdCl$_2$(dppe)]: LUMO-1

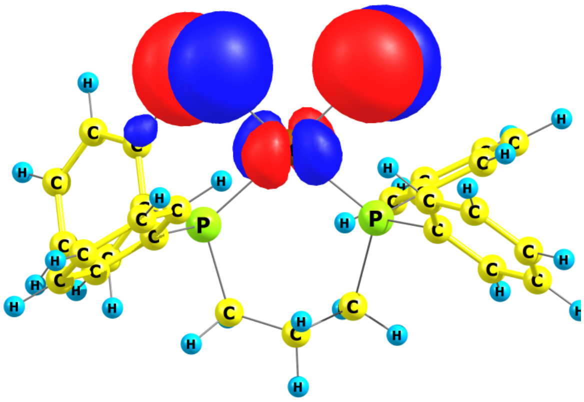

[PdCl$_2$(dppp)]: HOMO

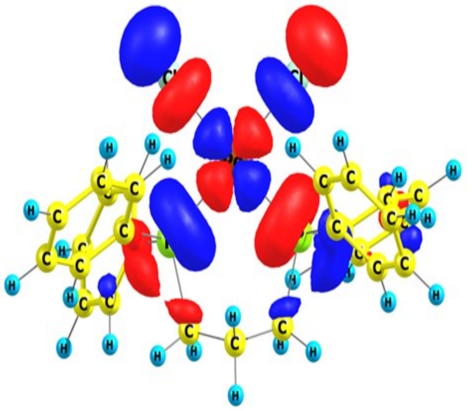

[PdCl$_2$(dppp)]: LUMO

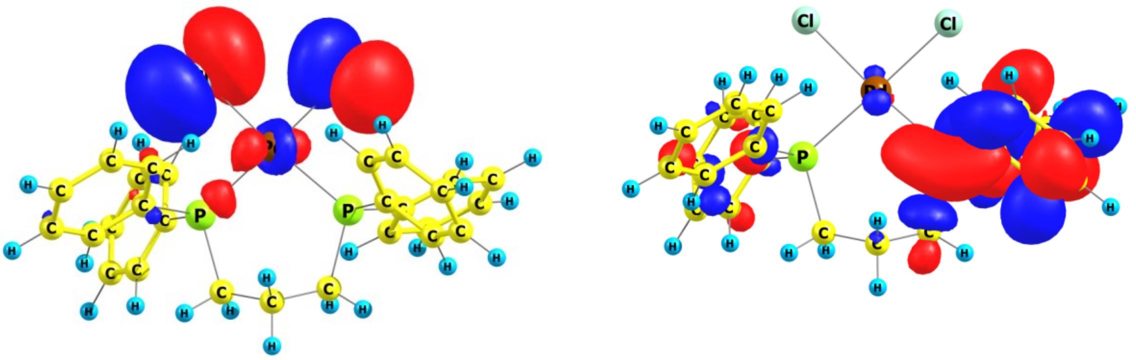

[PdCl$_2$(dppp)]: HOMO-1 **[PdCl$_2$(dppp)]: LUMO+1**

Figure 8: Frontier Molecular orbitals of [PdCl$_2$(P-P)] (P-P = PPh$_3$, dppm, dppe, dppp)

Since the reactivity of molecule is strongly correlated to electronic properties of molecule, electronic parameters like energy of HOMO and LUMO, chemical potential (μ), chemical hardness (η) and Fundamental gap of these two molecules were calculated and results are presented in **Table-8**. The energy difference in HOMO and LUMO (E_{LUMO}-E_{HOMO}) correlates with the reactivity of chemical species. Lower (E_{LUMO}-E_{HOMO}), value of separation energy, higher the reactivity attributed to that chemical species. The electronic chemical potential (μ) and chemical hardness (η) were calculated using energy of lowest unoccupied molecular orbital (E_{LUMO}) and the highest occupied molecular orbital (E_{HOMO}) as $\mu = (E_{HOMO} + E_{LUMO})/2$ and $\eta = (E_{HOMO} - E_{LUMO})/2$

The vertical electron affinity (EA_V) has been calculated as difference in the total energy of neutral and attained anion after addition of an electron on geometry of neutral. The vertical ionization energy (IE_v) was calculated as difference in total energy of attained cation after removal of electron from neutral (*keeping the geometry fixed*) and the neutral. The fundamental gap (E_{GAP}) was calculated as E_{GAP} = (IE_v) - (EA_V). The present work [PdCl$_2$(dppe)] shows a higher value of E_{LUMO}-E_{HOMO} energy and fundamental gap compared to other two chelating phosphine ligands, thereby suggesting lower reactivity/higher stability.

Table 8: Comparative prospects of various electronic properties in [$PdCl_2$(P-P)] (P-P = PPh_3, dppm, dppe, dppp)

	[$PdCl_2$(dppm)]	[$PdCl_2$(dppe)]	[$PdCl_2$(dppp)]
E_{HOMO}	-6.07	-6.05	-6.06
E_{LUMO}	-2.47	-2.25	-2.34
E_{HOMO} - E_{LUMO}	3.60	3.80	3.71
chemical potential (μ)	-4.27	-4.14	-4.20
chemical hardness (η)	1.80	1.89	1.85
EA_V	1.17	1.00	1.01
IE_v	7.43	7.46	7.38
Fundamental Gap	6.28	6.46	6.29

According to HSAB principles, nucleophilic and electrophilic species can be categorized as either "hard" or "soft" based on polarizability. Apart from this Hardness and softness are important factors for estimation of their reactivity because generally, electrophile (4,6-dimethyl pyrimidin-2-thiol) involved in substitution reaction of [$PdCl_2$(P-P)] (P-P = PPh_3, dppm, dppe, dppp) form adducts via electron-rich nucleophiles (*nucleophilic targets sulfide ion*). During the formation of bond, the electrophile molecule [Pd(ligand)$_4$ moiety] accepted an electron in its LUMO from the nucleophilic target 4,6-dimethyl pyrimidin-2-thiol (*nucleophilic targets sulfide ion*). The formation and strength of this covalent bond is governed by "hardness"/softness of molecules involved in reaction.

The presence of two additional methyl groups in 4,6-dimethyl pyrimidin-2-thiol provide it with additional electron density of sulfide ion and enhances its softness. The geometrical and electronic nature of 4,6-dimethyl pyrimidin-2-thiol and its parent analogue is quite similar as shown in **Figure S5 (Supplementary Information).**

Since the electrophilic molecule preferentially formed covalent adducts with nucleophiles of similar softness/hardness, the reactivity of molecule is correlated with its hardness. In case of present work, the stability and hardness of [$PdCl_2$(P-P)] (P-P = PPh_3, dppm, dppe, dppp) is quite different. In fact, the value of hardness of 4,6-dimethyl pyrimidin-2-thiol is comparable with dppm and quite far from the dppe. The reaction of [$PdCl_2$(dppm)] with two moles of Na{2-$SC_4H(4,6\text{-}Me)_2N_2$} resulted in a dimeric complex [$Pd_2(\mu_2\text{-}S)\{SC_4H(4,6\text{-}Me_2)_2N_2\}_2(\mu_2\text{-}dppm)_2$] may be attributed to higher reactivity and cleavage of S-C bond of Spym to afford S^2. The closer to 90° Pd(Ligand)$_4$ geometry provides stability to [$PdCl_2$(dppe)] and further its vast difference in degree of softness with nucleophile (4,6-dimethyl pyrimidin-2-thiol) results in controlled reactivity and results in *cis*-configured monomeric complex. For the case of [$PdCl_2$(dppp)], the steric hindrance/stiffness (*due to P-Pd-P angle closer to 100°, non-linearity in bridging C-C-C and pseudo staggered aryl rings*) present in its atomic geometry along with the degree of softness in its electronic structure may be attributed to relatively higher/rapid reactivity and complete removal of 'dppp' (1,3-bis(diphenylphosphino)propane) to form chelated complex [$Pd\{\kappa\text{-}S, \kappa\text{-}N: SC_4H(4,6\text{-}Me)_2N_2\}_2$] (**2c**) instead of mononuclear complex.

5. Conclusions

In current study, various complexes were isolated depending on the nature of phosphine. The bite angle projected by chelating phosphine played a crucial role in obtaining dimeric, monomeric and chelated complexes. Most importantly, reactivity of 4,6-dimethyl pyrimidine-2-thiol is significantly different compared to unsubstituted pyrimidyl, pyridyl derivatives of thiolate ligand systems. Probably, the presence of electron donating behavior of methyl group with structure made the ring electron rich and facilitated competitive reactivity pattern of S-S and S-C bond in 4,6-dimethylpyrimidine-2-thiolate ligand system. The virtue of such activation can easily be understood by the isolation of complex [$Pd_2(\mu_2\text{-}S)\{SC_4H(4,6\text{-}$

$Me_2)_2N_2\}_2(\mu_2\text{-dppm})_2]$. In order to have a better understanding about reactivity of $[PdCl_2(P\text{-}P)]$ (P-P = dppm, dppe, dppp) against 4,6-dimethylpyrimidine-2-thiolate, DFT studies were carried out. The findings reveal that bite angle projected by chelating phosphine and associated softness of molecule played a crucial role in obtaining dimeric, monomeric and chelated complexes. Projection angle P-M-P ranging from ~75 to 92° caused structural diversification which opened a new window for various researchers to explore this field further in order to derive biologically as well as academically important complexes.

6. Declaration of Competing Interest

The authors declare that they have no competing financial interests or personal relationships that could have appeared to influence the work reported in this paper.

Appendix A. Supplementary data

CCDC 2271550, 2269838, 2239423, 2231645 for complexes $[Pd\{\kappa\text{-S}, \kappa\text{-N}: SC_4H(4,6\text{-}Me)_2N_2\}\{SC_4H(4,6\text{-}Me)_2N_2\}(PPh_3)]$, $[Pt\{SC_4H(4,6\text{-}Me)_2N_2\}_2(PPh_3)_2]$, $[Pd_2(\mu_2\text{-}S)\{SC_4H(4,6\text{-}Me)_2N_2\}_2(\mu_2\text{-dppm})_2]$ and $[Pd\{\kappa\text{-S}, \kappa\text{-N}: SC_4H(4,6\text{-}Me)_2N_2\}_2]$ (**2c**) respectively contains the supplementary crystallographic data for this paper. These data can be obtained free of charge via http://www.ccdc.cam.ac.uk/data_request/cif, from the Cambridge Crystallographic Data Centre, 12 Union Road, Cambridge CB2 1EZ, UK; fax: (+44) 1223-336-033; or e-mail: deposit@ccdc.cam.ac.uk

Acknowledgements

One of the authors Dr. Afsar Ali Siddiki is thankful to DST-SERB for providing grant TARE/2022/000220 to carry out this work. Authors are also thankful to Mr. Kamlesh Sathpute (IIT Ropar) and V. Ramkumar (IIT Madras) for carrying out the single crystal XRD.

References

[1] T.S. Lobana, Heterocyclic-2-thione derivatives of group 10–12 metals: Coordination versatility, activation of CS (thione) bonds and biochemical potential, Coord. Chem. Rev. 441 (2021) 213884.

[2] V.K. Jain, Internally functionalized multifaceted organochalcogen compounds, Dalton Trans. 49(26) (2020) 8817-8835.

[3] P. Oswal, A. Arora, S. Gairola, A. Datta, A. Kumar, Organosulfur, organoselenium, and organotellurium ligands in the development of palladium, nickel, and copper-based catalytic systems for Heck coupling, New J Chem 45(46) (2021) 21449-21487.

[4] R. Cargnelutti, R.F. Schumacher, A.L. Belladona, J.C. Kazmierczak, Coordination chemistry and synthetic approaches of pyridyl-selenium ligands: A decade update, Coord. Chem. Rev. 426 (2021) 213537.

[5] S.V. Lokhande, A. Tyagi, R.J. Butcher, G. Karmakar, R.S. Chauhan, Study of an interesting interplay between thiourea and 4, 6-dimethylpyrimidine-2-thiol with palladium (II) phosphine substrate, Polyhedron 230 (2023) 116221.

[6] R.S. Chauhan, Reactivity of hemi-labile pyridyl and pyrimidyl derived chalcogen ligands towards group 10 metal phosphine precursors, New J Chem 44(7) (2020) 2689-2696.

[7] M.S. Lokolkar, M.K. Pal, S. Dey, B.M. Bhanage, POP-Pincer Xantphos Pd Complex of 4-Pyridylthiolate: Cyclocarbonylative Reaction for the Synthesis of Flavones Using Cobalt Carbonyl as a C1 Source, Catal. Lett. (2022).

[8] M.S. Lokolkar, P.A. Mane, S. Dey, B.M. Bhanage, Xantphos-coordinated palladium dithiolates: Highly efficient catalyst for decarboxylative Sonogashira reaction into corresponding alkynes, Appl. Organomet. Chem. 35(9) (2021) e6328.

[9] V.V. Gaikwad, P.A. Mane, S. Dey, D. Patel, B.M. Bhanage, Supramolecular Pd(II) complex of DPPF and dithiolate: An efficient catalyst for amino and phenoxycarbonylation using $Co_2(CO)_8$ as sustainable C1 source, Mol. Catal. 482 (2020) 110672.

[10] R.N. Prabhu, R. Ramesh, Catalytic application of dinuclear palladium (II) bis (thiosemicarbazone) complex in the Mizoroki-Heck reaction, Tetrahedron Lett. 53(44) (2012) 5961-5965.

[11] S. Kukunuri, K. Naik, S. Sampath, Effects of composition and nanostructuring of palladium selenide phases, Pd_4Se, Pd_7Se_4 and $Pd_{17}Se_{15}$, on ORR activity and their use in Mg–air batteries, Journal of Materials Chemistry A 5(9) (2017) 4660-4670.

[12] R.S. Chauhan, N. Shivran, Emerging trends in organotellurolate chemistry derived from platinoids, RSC Adv. 7(87) (2017) 55175-55198.

[13] G. Karmakar, A. Tyagi, G. Kedarnath, N. Naveen Kumar, P.P. Phadnis, R. Mishra, M. Kumar, Preparation and characterization of colloidal $Pd_{17}Se_{15}$ nanoparticles from a novel Pd(II) pyridyl selenoether molecular precursor, Inorganica Chim. Acta 529 (2022) 120668.

[14] S. Dey, K.V. Vivekananda, A.P. Wadawale, V.K. Jain, N. Bhuvanesh, Reactivity of 4-Pyridyltellurolate with Pd (II)/Pt (II) Complexes, ChemistrySelect 2(18) (2017) 5073-5079.

[15] S. Narayan, V.K. Jain, Platinum (II) pyridine-2-thiolate and-selenolate complexes, Transition Met. Chem. 24(4) (1999) 409-413.

[16] J.L. Serrano, J. Perez, G. Sanchez, J.F. Martínez, G. Lopez, E. Molins, Synthesis of S, N-chelating heterocyclic thionates of palladium (II). Crystal structure of *cis*-[Pd(pym-2-S)$(PPh_3)_2$](pym-2-S= pyrimidine-2-thionate), Transition Met. Chem. 27(1) (2002) 105-109.

[17] T.S. Lobana, R. Verma, G. Hundal, A. Castineiras, Metal–heterocyclic thione interactions.: 12. Heterocyclic 2-thiolates of platinum (II) and palladium (II): the crystal structures of first examples of *cis*-[M(η1-S-pyridine-2-thiolato)$_2$(LL)]{M = Pt, Pd, LL= 1,2-bis (diphenylphosphino) ethane; M = Pt, LL= 1, 2-bis(diphenylphosphino)ethene} complexes, Polyhedron 19(8) (2000) 899-906.

[18] M.K. Pal, A.G. Majumdar, K.V. Vivekananda, A.P. Wadawale, M. Subramanian, N. Bhuvanesh, S. Dey, Anticancer activity of Pt-selenolate metallacycles, New J Chem 46(48) (2022) 23198-23212.

[19] S. Miranda, E. Cerrada, A. Luquin, A. Mendía, M. Laguna, Palladium and platinum pyrimidine-2-thionate complexes with diphosphines, Polyhedron 43(1) (2012) 15-21.

[20] R.S. Chauhan, G. Kedarnath, A. Wadawale, A.M.Z. Slawin, V.K. Jain, Reactivity of 2-chalcogenopyridines with palladium–phosphine complexes: isolation of different complexes depending on the nature of chalcogen atom and phosphine ligand, Dalton Trans. 42(1) (2013) 259-269.

[21] G. Kedarnath, V.K. Jain, Pyridyl and pyrimidyl chalcogen (Se and Te) compounds: A family of multi utility molecules, Coord. Chem. Rev. 257(7) (2013) 1409-1435.

[22] A.Y. Kulkarni, S.V. Lokhande, A.A. Siddiki, R.S. Chauhan, R.J. Butcher, Scrambling of Metal Precursors: A Strategy to Synthesize Trinuclear $[M_3(\mu\text{-Se})_2(dppe)_3]^{2+}$ (M = Ni, Pd) and Pentanuclear $[Pd_5(\mu_3\text{-Se})_4(dppe)_4]^{2+}$ Coordination Clusters, J. Cluster Sci. (2023) 1-10.

[23] A.R. Sanger, Diphosphine complexes of iridium(I), palladium(II), and platinum(II), J. Chem. Soc., Dalton Trans. (20) (1977) 1971-1976.

[24] D. Xu, Z. Zhu, Z. Wang, A Convenient Synthesis of 4,6-Dimethyl-2-(Methylsulfonyl)Pyrimidine, J. Chem. Res. 37(12) (2013) 720-721.

[25] G.M. Sheldrick, SHELXT–Integrated space-group and crystal-structure determination, Acta Crystallogr. A: Found. Adv. 71(1) (2015) 3-8.

[26] G.M. Sheldrick, Crystal structure refinement with SHELXL, Acta Crystallogr. Sect.C: Struct. Chem. 71(1) (2015) 3-8.

[27] C.F. Macrae, I. Sovago, S.J. Cottrell, P.T. Galek, P. McCabe, E. Pidcock, M. Platings, G.P. Shields, J.S. Stevens, M. Towler, Mercury 4.0: From visualization to analysis, design and prediction, J. Appl. Crystallogr. 53(1) (2020) 226-235.

[28] W. Schmidt, K. K. Baldridge, J. A. Boatz, S. T. Elbert, M. S. Gordon, J. H. Jensen, S. Koseki, N. Matsunaga, K. A. Nguyen, J. S. Su, T. L. Windus, M. Dupuis, J. A. Montgomery , General atomic and molecular electronic structure system, J. Comput. Chem., 14 (1993) 1347-1363.

[29] A. D. Becke, Density-functional exchange-energy approximation with correct asymptotic behavior, Phys. Rev. A, 38 (1988) 3098-3100.

[30] C. Lee, W. Yang, R. G. Parr, Development of the Colle-Salvetti correlation-energy formula into a functional of the electron density, Phys. Rev. B, 37 (1988) 785-789.

[31] W.J. Hehre, R.F. Stewart, J.A. Pople, Self-consistent molecular-orbital methods. I. Use of Gaussian expansions of Slater-type atomic orbitals, J. Chem. Phys. 51(6) (1969) 2657-2664.

[32] W. Hehre, R. Ditchfield, R. Stewart, J. Pople, self-consistent molecular orbital methods. iv. use of Gaussian expansions of Slater-type orbitals. Extension to second-row molecules, J. Chem. Phys. 52(5) (1970) 2769-2773.

[33] M.S. Gordon, M.D. Bjorke, F.J. Marsh, M.S. Korth, Second-row molecular orbital calculations. 5. A minimal basis INDO for sodium-chlorine, J. Am. Chem. Soc. 100(9) (1978) 2670-2678.

[34] W.J. Stevens, H. Basch, M. Krauss, Compact effective potentials and efficient shared-exponent basis sets for the first-and second-row atoms, J. Chem. Phys. 81(12) (1984) 6026-6033.

[35] W.J. Stevens, M. Krauss, H. Basch, P.G. Jasien, Relativistic compact effective potentials and efficient, shared-exponent basis sets for the third-, fourth-, and fifth-row atoms, Can. J. Chem. 70(2) (1992) 612-630.

[36] T.R. Cundari, W.J. Stevens, Effective core potential methods for the lanthanides, J. Chem. Phys. 98(7) (1993) 5555-5565.

[37] R.S. Chauhan, R.K. Sharma, G. Kedarnath, D.B. Cordes, A.M.Z. Slawin, V.K. Jain, Reactivity of dipyrimidyldiselenides with [M(PPh$_3$)$_4$] and 2-pyrimidylchalcogenolates with [MCl$_2$(diphosphine)] (M = Pd or Pt), J. Organomet. Chem. 717 (2012) 180-186.

[38] S. Nadeem, M. Bolte, S. Ahmad, T. Fazeelat, S.A. Tirmizi, M.K. Rauf, S.A. Sattar, S. Siddiq, A. Hameed, S.Z. Haider, Synthesis, crystal structures and, antibacterial and antiproliferative activities in vitro of palladium(II) complexes of triphenylphosphine and thioamides, Inorganica Chim. Acta 363(13) (2010) 3261-3269.

[39] V.P. Ananikov, S.S. Zalesskiy, V.V. Kachala, I.P. Beletskaya, NMR approach for the identification of dinuclear and mononuclear complexes: The first detection of [Pd(SPh)$_2$ (PPh$_3$)$_2$] and [Pd$_2$(SPh)$_4$(PPh$_3$)$_2$]–The intermediate complexes in the catalytic carbon–sulfur bond formation reaction, J. Organomet. Chem. 696(1) (2011) 400-405.

[40] C.P. Morley, C.A. Webster, M. Di Vaira, Oxidative addition of (PhSe)$_2$ and (FcSe)$_2$ to zerovalent palladium and platinum trialkylphosphine complexes (Fc = ferrocenyl,[Fe (η5-C$_5$H$_5$)(η5-C$_5$H$_4$)]), J. Organomet. Chem. 691(20) (2006) 4244-4249.

[41] R. Oilunkaniemi, R.S. Laitinen, M. Ahlgrén, The NMR spectroscopic and X-ray crystallographic study of the oxidative addition of bis (2-thienyl) diselenide to zerovalent palladium and platinum centers, J. Organomet. Chem. 587(2) (1999) 200-206.

[42] T.S. Lobana, R. Verma, A. Castineiras, The chemistry of pyridine thiols and related ligands—8. Synthesis, NMR spectroscopy and crystal structure of first *trans*-[bis (pyridine-2-thiolato-S)-bis (triphenyl phosphine) platinum (II)], Polyhedron 17(21) (1998) 3753-3758.

[43] A. Mendía, E. Cerrada, F.J. Arnáiz, M. Laguna, Pyridine-2-thionate as a versatile ligand in Pd(II) and Pt(II) chemistry: the presence of three different co-ordination modes in [Pd$_2$(μ$_2$-S,N-C$_5$H$_4$SN)(μ$_2$-κ$_2$S-C$_5$H$_4$SN)(μ$_2$-dppm)(S-C$_5$H$_4$SN)$_2$], Dalton Trans. (4) (2006) 609-616.

[44] R.S. Chauhan, C.P. Prabhu, P.P. Phadnis, G. Kedarnath, J.A. Golen, A.L. Rheingold, V.K. Jain, Oxidative addition reactions of nicotinamide based organoselenium compounds on [M

$(PPh_3)_4$](M= Pd or Pt): An insight study for the formation of several isolable products, J. Organomet. Chem. 723 (2013) 163-170; R. S. Chauhan, A. Kumar, P. Prabhu, Synthesis of palladium tellurolate complexes derived from hemi-labile tellurolate ligands and studies their reactivity as gas sensing materials, Inorganica. Chim. Acta 487 (2019) 365-397.

[45] T.S. Lobana, A.K. Sandhu, R.K. Mahajan, G. Hundal, S.K. Gupta, R.J. Butcher, A. Castineiras, Dinuclear PdII/PtII complexes [M_2(phosphine)n(thio-ligand)$_3$]Cl incorporating N,S-bridged pyridine-2-thiolate and benzimidazoline-2-thiolate, Polyhedron 127 (2017) 25-35.

[46] A. Balch, B. IS, Novel reactions of metal-metal bonds. addition of sulfur dioxide and sulfur to $Pd_2(Ph_2PCH_2PPh_2)_2Cl_2$ and the oxidation of coordinated sulfide, (1979).

[47] G. Besenyei, L. Parkanyi, L.I. Simandi, B.R. James, Synthesis and Characterization of Dinuclear Palladium Complexes with Bridging Selenide or Selenoxide Ligands, Including X-ray Characterization of anti-$Pd_2Cl_2(\mu\text{-}Se)(\mu\text{-}dpmMe)_2$ [dpmMe = 1,1-Bis(diphenylphosphino)ethane], Inorg. Chem. 34(24) (1995) 6118-6123.

[48] K. Umakoshi, I. Kinoshita, A. Ichimura, S. Ooi, Binuclear platinum(II) and -(III) complexes of pyridine-2-thiol and its 4-methyl analog. Synthesis, structure, and electrochemistry, Inorg. Chem. 26(21) (1987) 3551-3556.

[49] S. Ahmad, T. Rüffer, H. Lang, S. Nadeem, S. Tirmizi, M. Saleem, A. Anwar, Synthesis, crystal structure, and antimicrobial studies of *trans*-[Pd$(PPh_3)_2$(imidazolidine-2-thione)$_2$]Cl_2· 3.5 H_2O, Russ. J. Coord. Chem. 36 (2010) 520-524.

[50] R.S. Chauhan, G. Kedarnath, A. Wadawale, A. Munoz-Castro, R. Arratia-Perez, V.K. Jain, W. Kaim, Tellurium (0) as a ligand: synthesis and characterization of 2-pyridyltellurolates of platinum (II) and structures of [Pt{2-Te-3-(R) C5H_3N}$_2$Te (PR′$_3$)](R = H or Me), Inorg. Chem. 49(9) (2010) 4179-4185; R. S. Chauhan, D. Oza, S. Nigam, A. Tyagi, S. Ansari, R. J. Butcher, C. Dash, Reactivity of hemilabile 2-pyridylselenolate ligand towards [$NiCl_2$(dppe)]: Combined experimental and theoretical study, J. Mol. Struct. 1248 (2022) 131368.

[51] P. A. Papanikolaou, A. G. Papadopoulos, A. Hatzidimitriou, P. Aslanidis, Neutral mononuclear luminescent Pd (II) complexes with heterocyclic thiolate ligands and chelating phosphines. Structural and photophysical assignments. Polyhedron, 94 (2015) 67-74.